NASA TECHNICAL NOTE

NASA TN D-7225

NASA TN D-7225

EVALUATION OF AN EXPERIMENTAL SHORT-LENGTH ANNULAR COMBUSTOR: ONE-SIDE-ENTRY DILUTION AIRFLOW CONCEPT

by Francis M. Humenik and James A. Biaglow

Lewis Research Center
Cleveland, Ohio 44135

NATIONAL AERONAUTICS AND SPACE ADMINISTRATION • WASHINGTON, D. C. • MARCH 1973

1. Report No.	2. Government Accession No.	3. Recipient's Catalog No.
NASA TN D-7225		

4. Title and Subtitle	5. Report Date
EVALUATION OF AN EXPERIMENTAL SHORT-LENGTH ANNULAR COMBUSTOR: ONE-SIDE-ENTRY DILUTION AIRFLOW CONCEPT	March 1973
	6. Performing Organization Code
7. Author(s) Francis M. Humenik and James A. Biaglow	8. Performing Organization Report No. E-7267
	10. Work Unit No. 501-24
9. Performing Organization Name and Address Lewis Research Center National Aeronautics and Space Administration Cleveland, Ohio 44135	11. Contract or Grant No.
	13. Type of Report and Period Covered Technical Note
12. Sponsoring Agency Name and Address National Aeronautics and Space Administration Washington, D.C. 20546	14. Sponsoring Agency Code

15. Supplementary Notes

16. Abstract

A test program was conducted to evaluate an experimental short-length annular combustor that uses a one-side-entry dilution airflow concept. The combustor design features scoops on the outer liner for controlling the primary- and secondary-zone airflow distribution. Combustor inlet total pressures were limited to 62 N/cm^2 (90 psia) with inlet-air temperatures from 590 K (600° F) to 890 K (1150° F). At a diffuser inlet Mach number of 0.25, the exit-temperature pattern factor was 0.44 with an average exit temperature of 1436 K (2124° F) and a total pressure loss of 4.3 percent. At a diffuser inlet Mach number of 0.31, the exit-temperature pattern factor was reduced to 0.29 with an average exit temperature of 1450 K (2151° F) and a total pressure loss of 6.1 percent. Nominal combustion efficiencies of 100 percent were obtained with the ASTM A-1 fuel. Exhaust gas emissions, smoke, and altitude relight data are included with exit-temperature profiles and distribution patterns.

17. Key Words (Suggested by Author(s))	18. Distribution Statement
Short-length combustor Side-entry combustor Exhaust emissions Dilution airflow concept	Unclassified - unlimited

19. Security Classif. (of this report)	20. Security Classif. (of this page)	21. No. of Pages	22. Price*
Unclassified	Unclassified	46	$3.00

* For sale by the National Technical Information Service, Springfield, Virginia 22151

EVALUATION OF AN EXPERIMENTAL SHORT-LENGTH ANNULAR COMBUSTOR: ONE-SIDE-ENTRY DILUTION AIRFLOW CONCEPT

by Francis M. Humenik and James A. Biaglow

Lewis Research Center

SUMMARY

A test program was conducted to evaluate an experimental short-length annular combustor that uses a one-side-entry dilution airflow concept. The combustor design features scoops on the outer liner for controlling the primary- and secondary-zone airflow distribution. Combustor inlet total pressures were limited to 62 N/cm^2 (90 psia) with inlet-air temperatures from 590 K (600° F) to 890 K (1150° F). At the simulated sea-level takeoff condition a high exit-temperature pattern factor of 0.44 limited testing to an average exit temperature of 1436 K (2124° F). For the Mach 3.0 cruise condition, a pattern factor of 0.29 was obtained with an average exit temperature of 1450 K (2151° F). The total pressure losses were 4.3 percent and 6.1 percent, respectively, for these test conditions. Nominal combustion efficiencies of 100 percent were obtained with the ASTM A-1 fuel used for all testing.

A high smoke number of 72 and an oxides-of-nitrogen emission index of 4.2 grams per kilogram of fuel were obtained for inlet airflow test conditions simulating sea-level takeoff at a reduced pressure level. The smoke number decreased to 26 and the oxides-of-nitrogen emission index increased to 12.5 grams per kilogram of fuel for inlet airflow test conditions simulating Mach 3.0 cruise operation. At airflow conditions simulating idle operation of a high-pressure ratio subsonic engine the combustion efficiency was near 100 percent, resulting in low exhaust pollutant levels for carbon monoxide and unburned hydrocarbons.

Combustor altitude relight was obtained at an inlet pressure of 2.8 N/cm^2 (4.1 psia) with ambient inlet-air temperature of 294 K (70° F).

INTRODUCTION

This report presents performance data, including exhaust gas emission levels, for an experimental short-length annular combustor. This combustor design incorporates a one-side-entry dilution airflow concept.

Advanced jet aircraft engines (refs. 1 and 2) operate under conditions which produce a wide range of compressor exit airflow profiles. These varying airflow profiles can distort the exit-temperature distribution of a combustor and adversely affect the performance and life of an engine. What is needed is a combustor design insensitive to changes in the compressor exit airflow profile. One concept that has shown promise as being insensitive to distorted airflow profiles is the one-side-entry combustor (ref. 3). This combustor has a "side entry" type design which uses primary and secondary air scoops on only the outer diameter side to inject high-velocity airflow into the combustor. Previous rectangular segment tests of the design satisfactorily demonstrated its concept and are described in references 3 and 4. In the segment tests, intentionally distorting the diffuser inlet radial airflow profile did not cause any undesirable shift in the radial exit-temperature profile. Other side-entry-type combustor designs are described in references 5 and 6. Diffuser devices for correcting radial airflow distortions are suggested in reference 7.

An advanced jet engine combustor test facility described in reference 8 afforded the capability to investigate the full-annular, three-dimensional flow field of a one-side-entry combustor at air pressures and temperatures simulating actual engine conditions. Full-annulus tests are necessary because practical hardware problems such as optimum ignitor location, fuel strut installation techniques, and combustor scaling may require design adjustments. In addition, sidewall effects that occur in rectangular segment tests are eliminated, simulation of the diffuser airflow passage can be exact, and radial and circumferential airflow distribution effects can be studied.

The combustor was designed for an average exit temperature of 1478 K (2200° F) using ASTM A-1 fuel. Inlet total pressure was set at 62 N/cm^2 (90 psia), and inlet total temperature varied from 590 K (600° F) to 890 K (1150° F). Diffuser inlet Mach numbers ranged from 0.24 to 0.32 for test conditions from simulated sea-level takeoff to Mach 3.0 cruise operation. Performance data that were obtained included combustion efficiency, pressure loss, exit-temperature distributions, and exhaust emissions. These data are presented for an outer-liner design with primary scoops sized for 30 percent of total airflow. Idle and altitude relight data are presented for two outer-liner designs with primary scoops sized for 25 percent of total airflow. The inlet velocity profiles were not distorted for the data presented in this report.

COMBUSTOR DESIGN

Side-Entry Concept

The design concept investigated in this test program is referred to as a side-entry combustor and is shown in figure 1. It is an annular combustor with most of the airflow injected through an outer-liner wall. Small amounts of airflow are used for cooling of an inner-liner wall and a firewall, with additional air for swirling with the liquid fuel injected by pressure atomizing nozzles. Scoops attached to the outer-liner wall apportion diffuser airflow between the primary combustion zone and the secondary dilution zone. These scoops extend to the full height of the annular passage so that an entire radial velocity airflow sample is captured. Thus, regardless of radial profile distortion, the combustor airflow distribution does not change. This results in a stable radial exit-temperature profile at the combustor exit.

Combustor Design Details

The full-annulus side-entry combustor and associated diffuser design used for this investigation are shown in cross section in figure 1. The diffuser passage contour selected had a steep inner diffuser wall angle of about 50°, as compared to an inner wall angle of about 24° that was used in the segment tests described in reference 3. This provided additional outer-liner length of about 5 centimeters (2 in.) for possible air entry position adjustment. The design exit-to-inlet area ratio of 1.8 was equivalent to the segment area ratio. Individual inlet chutes, the full height of the diffuser passage, were located between each of 32 fuel nozzle positions. These chutes supplied about 18 percent of the total airflow to the inner liner and firewall for cooling and swirler flows.

Fuel struts were assembled with the parts shown in figure 2. Either a radial or an axial swirler could be used with this assembly. The radial air swirler which had eight turning vanes was selected for the final series of tests. A closeup view of the final assembly is shown in figure 3. The minimum flow area for each swirler was 7.87 square centimeters (1.22 in.^{2}).

Outer-liner designs. - Several outer-liner designs were evaluated in preliminary testing of this combustor concept. The liner design that was used for evaluating the combustor exit temperature distribution is designated as liner 3 and is shown in figure 4. A set of 32 scoops injected the primary airflow. A set of 32 secondary scoops, downstream and in line with the primary scoops, were attached to a set of secondary slots (set 1, fig. 4) for dilution jet penetration to the hub region. A second set of secondary slots (set 2, fig. 4) were staggered between the first set of secondary slots for shallow penetration and tip cooling. Airflow to secondary slot set 2 was supplied by the set of hood

slots shown in figure 5. The gaps between the secondary scoops (normal supply path) were completely blocked in an attempt to improve circumferential airflow distribution. Short turning vanes along the sides of the secondary slots in set 2 were used for liner cooling between adjacent slots.

This design differed from the final rectangular segment design of reference 3. Primary scoop width was increased to flow 30 percent of the total airflow, as compared to about 21 percent in the segment design. Also, the set of hood slots were not used previously. These slots do not capture an entire radial velocity airflow sample and thus violate the original design concept. However, their use with uniform inlet airflow profiles was considered acceptable.

Preliminary liner designs 1 and 2, which had primary scoops sized for approximately 25 percent of total airflow, were used for altitude relight tests. Liner design 2 was also used to obtain some engine-idle emission data.

Approximately 82 percent of the total airflow was supplied to the outer liner. Design details for liners 1, 2, and 3 are listed in table I. The final combustor assembly with nominal airflow splits and pertinent flow areas is shown in figure 6.

Fuel nozzles. - Pressure atomizing simplex fuel nozzles were used in this investigation. Two fuel flow ranges were required. A high-flow-range set of nozzles was used for the sea-level takeoff, cruise, and idle test conditions; a low-flow-range set of nozzles was used for the altitude relight tests. Curves of total fuel flow for the combustor (sum of 32 nozzles) as a function of the differential pressure across the fuel nozzles are shown in figure 7.

APPARATUS AND PROCEDURE

Test Facility

The full-scale side-entry combustor investigation was conducted in a connected-duct test facility. A line diagram of this facility is shown in figure 8(a). An isometric sketch of typical combustor installation is shown in figure 8(b). Airflow rates and combustor pressures were regulated by remotely controlled valves upstream and downstream of the test section. Combustor inlet-air temperatures up to 922 K (1200° F) could be obtained without vitiation.

Additional figures, photographs, and descriptions of the facility are contained in references 8 to 10.

Instrumentation

Combustor inlet pressures and temperatures were measured at the locations shown in figures 9 and 10. Combustor exit total pressures and total temperatures were measured at 3° circumferential increments by three equally spaced traversing five-point probes. Airflow rates were measured with an orifice installed in accordance with ASME specifications. Fuel flow rates were measured with turbine-type flowmeters. Thorough descriptions of the traversing combustor exit probe system and of the data acquisition and recording system are contained in references 8 and 9.

Combustor exhaust emissions were sampled by means of two five-point water-cooled probes located 120° apart at the combustor exit. One probe was used for gas analysis samples and the other for smoke samples. The gas analysis system detected concentrations of nitric oxide, carbon monoxide, carbon dioxide, and unburned hydrocarbons. Details of the sampling probes and of the smoke and gas sampling systems are contained in the appendix.

Calculations

Combustion efficiency. - Efficiency was determined by dividing the measured temperature rise across the combustor by the theoretical temperature rise. The indicated readings of all thermocouples were taken as true values of the total temperatures. The exit thermocouples were high-recovery aspirating platinum - 13-percent rhodium/platinum (ref. 11, type 6). The exit temperatures were mass weighted for the efficiency calculation by the procedure given in reference 9. In each mass-weighted average, 585 individual exit temperatures were used.

Reference velocity and Mach number. - Reference conditions were based on the total airflow, the inlet-air density using the total pressure and temperature at the diffuser inlet, and the reference area (6270 cm^2 (972.5 $in.^2$)) as measured between the outer-liner hood diameter and the centerbody wall diameter at the diffuser exit plane. However, reference Mach numbers for altitude relight tests were based on a standard combustor reference area of 4484 square centimeters (695 $in.^2$) to simulate the conditions used for the advanced annular combustor described in reference 10.

Total pressure loss. - Combustor total pressure loss was calculated by mass-averaging 40 total pressures measured upstream of the diffuser inlet and 585 total pressures measured at the combustor exit. The combustor total pressure loss therefore includes the diffuser loss.

Diffuser inlet Mach number. - Diffuser inlet static pressure and total temperature with total airflow and inlet annulus area (1182 cm^2 (183.12 $in.^2$)) were used for calculating the inlet Mach number.

Radial profile factors. - The radial exit-temperature profile is established from the circumferential average of the temperature at each radial position and is plotted as a deviation from the average exit temperature against radial position. To detect temperature nonuniformities which may not be evident in the average radial profile, three temperature-profile quality factors were calculated; they are exit-temperature pattern factor $\bar{\delta}$, stator factor δ_{stator}, and rotor factor δ_{rotor}.

The exit-temperature pattern factor $\bar{\delta}$ was used to reflect the magnitude of nonuniformity caused by the maximum local temperature. This factor is defined as

$$\bar{\delta} = \frac{T_{max} - T_{av}}{\Delta T_{av}} \tag{1}$$

where T_{max} is the maximum individual exit temperature, T_{av} is the mass-weighted average exit temperature, and ΔT_{av} is the temperature difference between the mass-weighted average exit temperature and the average inlet temperature. To measure the magnitude of temperature nonuniformity which affects turbine stator vanes, a stator factor δ_{stator} was defined as

$$\delta_{stator} = \frac{(T_{R,max} - T_{R,design})_{max}}{\Delta T_{av}} \tag{2}$$

To measure the magnitude of temperature nonuniformity which affects turbine rotor blades, a rotor factor δ_{rotor} was defined as

$$\delta_{rotor} = \frac{(T_{R,av} - T_{R,design})_{max}}{\Delta T_{av}} \tag{3}$$

In these equations, $T_{R,max}$ is an individual maximum radial temperature, and $T_{R,av}$ is an average radial temperature which when compared to corresponding design radial average temperatures $T_{R,design}$, respectively, yields the maximum positive temperature differences and largest radial profile factors.

Units

The U.S. customary system of units was used for primary measurements and calculations. Conversion to SI units (System International d'Unites) was done for reporting

purposes only. In making the conversion, consideration was given to implied accuracy and may result in rounding off the values expressed in SI units.

Test Conditions

Test conditions were similar to those used in references 9 and 10 for an advanced annular combustor designed for Mach 3.0 cruise operation in engines having low compressor pressure ratios of about 14. Because of facility airflow limitations, reduced inlet-air total pressures were used to get the required diffuser inlet Mach number for sea-level takeoff simulation. Test conditions for Mach 3.0 cruise, simulated takeoff, and intermediate inlet-air temperatures are listed in table II.

The only idle conditions attempted were representative of an engine for subsonic cruise having a high compressor pressure ratio of about 24. These test conditions are inlet-air total pressure, 41 N/cm^2 (60 psia); inlet-air temperature, 480 K (400° F); airflow rate, 40 kg/sec (89 lb/sec); and fuel-air ratio, 0.008.

For altitude relight testing, the procedure used was similar to that described in reference 10. Pressures, temperatures, and airflow rates were set to simulate the required reference Mach number.

RESULTS AND DISCUSSION

Side-entry-combustor performance data including exit-temperature distributions, pressure loss, and exhaust emissions are presented for outer-liner configuration 3. Other data (not obtained with liner 3) were available for preliminary liners 1 and 2. Thus, engine-idle emission data are presented for liner 2, and altitude relight data are presented for outer-liner configurations 1 and 2. These data are listed in tables III, IV, and V. Significant performance characteristics are discussed in the following paragraphs.

Exit-Temperature Characteristics

Pattern factor. - One of the first requirements for good combustor performance is uniformity in the exit-temperature distribution pattern. Only small temperature deviations from the average exit temperature can be tolerated. This requires careful control of the radial and circumferential exit-temperature profiles. A measure of this control is obtained by calculating an exit-temperature pattern factor $\overline{\delta}$, which is a ratio which

reflects the difference between the maximum local temperature and the average exit temperature.

Low pattern factors in the 0.20 range indicate good exit-temperature distribution and uniformity with no undesirable hot spots. The pattern factor data for the side-entry combustor are listed in table III. These data are also presented in figure 11, which shows the pattern factor variation with average exit temperature for several inlet-air temperatures. The lowest (best) pattern factors, 0.27 to 0.37, were obtained with an inlet-air temperature of 750 K (900° F). High pattern factors, 0.35 to 0.48, were obtained with an inlet-air temperature of 590 K (600° F). At 890 K (1150° F) inlet-air temperature, the pattern factor was 0.29 with a mass-weighted average exit temperature of 1450 K (2151° F). At 590 K (600° F) inlet-air temperature, the pattern factor was 0.44 with a mass-weighted average exit temperature of 1436 K (2124° F). Thus, further development effort would be required to reduce these pattern factors and improve the exit-temperature distribution.

The location and severity of concentrated hot zones in the combustor exhaust can be shown by plotting average circumferential temperatures. Any zone which exceeds the overall average exit temperature by more than 10 percent of the temperature rise for the combustor usually yields excessive local temperatures. The characteristic average circumferential temperature profiles are shown in figure 12(a) for sea-level takeoff and in figure 12(b) for cruise conditions. The smaller temperature rise for cruise conditions resulted in less severe hot zones and lower pattern factors. The circumferential variation of the profiles indicates some tendency to form alternate hot and cold zones. Improved circumferential exit temperature uniformity is obviously necessary.

An annular display of the exit-temperature distribution by pattern factor zones yields a map similar to a plot of temperature isotherms, as shown in figure 13. Computer interpolations between adjacent exit-temperature measurements are transformed into pattern factor increments. Grouping of zones in accordance with the pattern factor letter and number code shows the characteristic gradients around the annulus. Typical characteristics for the final outer-liner configuration are shown in figure 13(a) for sea-level takeoff and in figure 13(b) for Mach 3.0 cruise conditions.

Numbered zones represent temperatures less than the overall average, whereas lettered zones represent temperatures greater than the overall average. An ideal (well mixed) combustor output would have relatively few temperature gradient lines. From this display of the pattern factor map, it is apparent that improved mixing is necessary to obtain good exit-temperature uniformity.

Another illustration of exit-temperature distribution by pattern factor range is shown in figure 14 as a histogram. This distribution (run 357, table III) is typical for sea-level takeoff conditions with an average exit temperature of 1436 K (2124° F). Only nine individual temperatures out of the total of 585 measurements were above a temperature level that would produce a pattern factor of 0.30, and only 12 were above a temperature level

that would produce a pattern factor of 0.25. Ideally, a narrow band or grouping of temperatures is desirable since this reflects optimum uniformity of temperature output.

Radial profile factors. - The design radial exit-temperature profile is determined from turbine stress considerations. Actual proximity to the design radial profile is measured by calculating stator and rotor factors for the exit-temperature distribution. The rotor factor is calculated from radial profile temperature differences. The stator factor is calculated from individual (local) temperature differences. Since high temperatures cause turbine stator and rotor deterioration, only positive values for these factors are of concern.

The radial profile obtained for sea-level takeoff conditions is shown in figure 15(a). The mass-weighted average exit temperature was 1436 K (2124° F) with a radial profile temperature difference of 38 K (68° F), corresponding to a rotor factor of only 0.045. However, because of an individual (local) temperature difference of 334 K (601° F), the stator factor was 0.397.

The radial profile obtained for Mach 3.0 cruise conditions is shown in figure 15(b). The mass-weighted average exit temperature was 1450 K (2151° F) with a radial profile temperature difference of 39 K (71° F), corresponding to a rotor factor of 0.071. An individual (local) temperature difference of 160 K (288° F) produced a stator factor of 0.289.

A radial exit-temperature profile adjustment to correct the cold-tip characteristic could probably have been accomplished by techniques such as covering the hood slots and removing the secondary blockage between scoops. However, the potential improvement did not warrant further development effort. Thus, no radial profile adjustment was attempted with outer-liner configuration 3.

Radial profile insensitivity. - Some data were obtained with inlet airflow profiles radially distorted by diffuser inlet flow trip rings. These data with liner 3 revealed some shift in the radial exit-temperature profile when a tip-peaked radial inlet airflow profile was used. The shift was attributed to increased airflow through the liner hood slots. Thus, control of the secondary airflow split was not maintained, resulting in a substantially colder tip region. Further development of the liner (including elimination of the use of hood slots) would be required to demonstrate the insensitivity concept of this combustor design.

Combustion Efficiency

Combustion efficiency data with combustor inlet pressures of 62 N/cm^2 (90 psia) are included in table III(a). Computed combustion efficiencies were nominally 100 percent over the range of fuel-air ratios from 0.011 to 0.024. The percentage variation among these data was very small. Characteristic trends with increasing fuel-air ratio were

insignificant. Additional data at low pressures (less than atmospheric) are included as part of the altitude relight performance listed in table V.

Total Pressure Loss

Total pressure loss data for outer-liner configuration 3 are included in table III. The combustor total pressure loss expressed as the percent of the average diffuser inlet total pressure is shown as a function of the diffuser inlet Mach number in figure 16. The two curves shown are data obtained without combustion (isothermal) and with a combustor temperature rise of about 556 K (1000° F). For a sea-level takeoff condition with an inlet Mach number of 0.25 and an average exit temperature of 1436 K (2124° F), the combustor total pressure loss was 4.3 percent. For a Mach 3.0 cruise condition with an inlet Mach number of 0.31 and an average exit temperature of 1450 K (2151° F), the combustor total pressure loss was 6.1 percent.

Exhaust Emissions: Simulated Cruise and Takeoff

A summary of the combustor exhaust smoke and gas emissions for liner configuration 3 is included in table III(b). The data cover a variety of exit temperatures for inlet-air temperatures from 590 K (600° F) to 890 K (1150° F). The gaseous exhaust emissions for nitric oxide (NO), total oxides of nitrogen (NO + NO_2), unburned hydrocarbons, carbon monoxide, and carbon dioxide are presented in terms of emission index (grams of constituent per kilogram of fuel) and parts per million by volume (ppm). Included in the table as a check on sample validity are the fuel-air ratios as determined by exhaust emissions and the fuel-air ratio as determined by separately measured flow rates of air and fuel. Smoke densities are presented in terms of a smoke number as defined in reference 12.

Oxides of nitrogen. - The measured values of emission index for oxides of nitrogen (NO + NO_2) varied from 4.2 grams of NO_2 per kilogram of fuel at simulated sea-level takeoff conditions (inlet-air temperature of 590 K (600° F); average exit temperature of 1436 K (2124° F)) to 12.5 grams per kilogram of fuel at Mach 3.0 cruise conditions (890 K (1150° F) inlet air temperature; average exit temperature of 1450 K (2151° F)). Figure 17 shows the effect of increasing exit temperature for different inlet-air temperatures on the formation of oxides of nitrogen. The fairly constant emission index at any of the inlet-air temperatures was caused by increasing volumetric concentrations being canceled out by equally increasing fuel-air ratios. Supplemental test data for 590 K (600° F) inlet-air temperature are included in figure 17 to show the spread in sample reproducibility for different days.

The effect of increasing inlet-air temperatures on the oxides-of-nitrogen formation for a nominal fuel-air ratio of 0.016 is shown in figure 18. The increase of oxides of nitrogen with increasing inlet-air temperatures agrees with the trend previously reported in reference 13.

Values of the emission index for nitric oxide are listed in table III(b) and account for 85 to 95 percent of the total concentration of oxides of nitrogen.

Unburned hydrocarbon emissions. - The concentration of unburned hydrocarbons as determined by the flame ionization detector was below the instrument accuracy on its most sensitive scale (±1 percent of 5 ppm C). The "C" denotes that the assumed form of unburned hydrocarbons were molecules of CH_2. The extremely low instrument readings necessitated a careful check of the operating and sampling procedure for sources of error. It was determined that the calibration procedure and the concentration of span and zero gases were such that accurate readings below 1 ppm C were impractical. Therefore, values of unburned hydrocarbons are listed in table III(b) as being present in concentrations of less than 1 ppm C.

Carbon monoxide emissions. - Emission index data for carbon monoxide are listed in table III(b); they varied from a high of 29.3 to a low of 3.3 grams per kilogram of fuel. At simulated sea-level takeoff conditions (run 357), the carbon monoxide emission index was 21.8 grams per kilogram of fuel. At Mach 3.0 cruise conditions (run 373), the carbon monoxide emission index decreased to 5.0 grams per kilogram of fuel. The effect of increasing inlet-air temperature for a variety of exit temperatures is shown in figure 19. Two emission curves for 590 K (600° F) inlet-air temperature are shown in this figure and indicate the sample reproducibility obtained when the data were repeated on different days. The effect of increasing inlet-air temperatures for a nominal fuel-air ratio of 0.016 is shown in figure 20. A steady decrease in carbon monoxide emissions is noted as the combustor inlet temperature is increased.

Sample validity. - Measured values of CO, CO_2, and hydrocarbons were used to determine a gas sample fuel-air ratio $(f/a)_{gs}$ to compare with fuel/air ratios determined by separately measured flow rates of fuel and air $(f/a)_m$. Agreement between the two fuel-air ratios would indicate how well the gas sampling probe was obtaining a representative sample of exhaust products. Gas sample fuel-air ratios within ±15 percent of measured values are considered to be an acceptable representation of the exhaust emissions, based on the sampling recommendations of reference 14.

Values of gas sample fuel-air ratios varied from 64 to 90 percent of measured fuel-air ratios and are listed in table III(b). Poorest agreement was obtained at 590 K (600° F) inlet-air temperature in which the gas sample values varied between 64 and 78 percent of the measured values. Increasing the inlet-air temperature to 750 K (900° F) improved the percentage agreement to between 82 and 84 percent. However, it was at inlet-air temperatures of 840 K (1050° F) and 890 K (1150° F) that the most representative samples of 85 to 90 percent were obtained. Increased mixing due to higher

reference velocities (note pattern factor improvement in fig. 11) produced the acceptable ratios at the higher inlet-air temperatures. The discrepancy between the measured and sample fuel-air ratios was attributed to the single sampling location and to a circumferential variation in mixing as illustrated by the exit-temperature profiles of figure 12.

Smoke number. - The combustor exhaust smoke numbers obtained for a single combustor inlet total pressure of 62 N/cm^2 (90 psia) are shown in figure 21. The smoke numbers varied from the barely visible region of 26 to 27 at 890 K (1150° F) inlet-air temperature to regions of high visibility - with smoke numbers reaching 72.5 at inlet-air temperatures of 590 K (600° F). Large smoke numbers are an indication of local fuel-rich regions and insufficient mixing in the primary zone (ref. 2). No attempt was made to reduce the smoke concentrations of the combustor.

Exhaust Emissions: Simulated Idle

Pollution levels for liner 2 at simulated high-pressure-ratio-engine idle operating conditions of 41 N/cm^2 (60 psia) inlet pressure, 480 K (400° F) inlet temperature, and 0.008 fuel-air ratio are shown in figure 22. The low emission index levels of carbon monoxide, about 28.6, and unburned hydrocarbons, about 3.4, are consistent with the high levels of combustion efficiency, near 100 percent, reported in table IV. The oxides of nitrogen shown in figure 22 varied from 2.37 to 3.00 grams per kilogram of fuel and agreed with the trend of liner 3 data toward low emission levels at reduced inlet-air temperatures. From inspection of the supplementary combustion efficiency data shown in table V with ambient inlet-air temperatures, it is reasonable to expect that high levels of combustion efficiency could also be obtained at idle conditions representative of a low-pressure-ratio engine.

Altitude Relight

Since outer-liner configuration 3 required further development effort to reduce pattern factor and improve exit-temperature distribution, no altitude relight data were obtained with this design. However, altitude relight data were available for previously tested outer-liner configurations 1 and 2 and are listed in table V(a).

In order to determine the optimum fuel-air ratio for relight, supplementary combustion efficiency data were obtained with ambient inlet-air temperatures for several inlet pressures below atmospheric. These data for liner 2 are listed in table V(b). Relight is most likely at fuel-air ratios which give maximum efficiency (usually at least 50 percent). Such efficiency data help to determine the optimum fuel flow rate for the most severe operating condition where combustion is still attainable.

The altitude relight data are shown in figure 23. It is apparent that the relight requirements for a Mach 3.0 type engine were easily met. With a reference Mach number of 0.10, relight was obtained at a combustor inlet pressure of 4.2 N/cm^2 (6.1 psia) and an inlet-air temperature of 300 K (80° F). With a reference Mach number of 0.05, relight was obtained at a combustor inlet pressure of 2.8 N/cm^2 (4.1 psia) and an inlet-air temperature of 294 K (70° F). The potential to operate at even more severe conditions than the minimum requirement appears feasible.

CONCLUDING REMARKS

Research on the one-side-entry combustor was initiated several years ago at NASA Lewis Research Center in rectangular segment tests. These segment tests showed good combustion efficiency, low pressure loss, good pattern factor, and insensitivity to inlet radial airflow distortion. Based on these results, a full annular combustor was constructed. Data from the annular combustor have shown good combustion efficiency; low pressure loss; and low levels of oxides of nitrogen, carbon monoxide, and unburned hydrocarbons. However, the full annular design has suffered from high pattern factors and has shown some sensitivity to distorted inlet radial velocity profiles with the use of outer-liner hood slots. Circumferential temperature plots and high levels of smoke have indicated that there is insufficient airflow and mixing in the primary zone. Elimination of these problems would require further liner development. The potential of the one-side-entry concept does not appear to be superior to other concepts under investigation, such as ram induction and swirl-can combustors; therefore, the research program on the side-entry combustor has been concluded.

SUMMARY OF RESULTS

A full-scale side-entry annular combustor was evaluated using ASTM A-1 fuel. Performance data were obtained with an outer-liner configuration having primary-zone scoops sized for 30-percent airflow. Altitude relight data were obtained with two outer-liner configurations having primary-zone scoops sized for 25-percent airflow. Inlet Mach numbers ranged from 0.24 to 0.32 for test conditions from simulated sea-level takeoff to Mach 3.0 cruise. Combustor inlet-air total pressure was 62 N/cm^2 (90 psia), and inlet-air temperatures ranged from 590 K (600° F) to 890 K (1150° F). The following results were obtained:

1. Localized hot streaks in the combustor exit-temperature distribution produced high pattern factors. For simulated takeoff conditions, the best (lowest) pattern factor with an average exit temperature of 1436 K (2124° F) was 0.44. For Mach 3.0 cruise

conditions, the best (lowest) pattern factor with an average exit temperature of 1450 K (2151° F) was 0.29.

2. Radial average exit-temperature profiles were reasonably good. At simulated sea-level takeoff conditions with an average exit temperature of 1436 K (2124° F), the highest positive average temperature deviation from the desired radial profile was 38 K (68° F), corresponding to a rotor factor of only 0.045. At cruise conditions with an average exit temperature of 1450 K (2151° F), the highest positive average temperature deviation from the desired radial profile was 39 K (71° F), corresponding to a rotor factor of 0.071. For these same conditions, individual (local) positive temperature deviations from the desired radial profile of 334 K (601° F) and 160 K (288° F) produced stator factors of 0.397 and 0.289, respectively.

3. The isothermal total pressure losses were 4.1 percent at an inlet Mach number of 0.25 and 5.9 percent at inlet Mach number of 0.31. With burning, the total pressure losses were 4.3 percent at an inlet Mach number of 0.25 (simulated sea-level takeoff condition) and 6.1 percent at an inlet Mach number of 0.31 (Mach 3.0 cruise conditions).

4. Computed combustion efficiencies nominally were 100 percent for simulated sea-level takeoff and cruise conditions with negligible variation (less than 1 percent) over the range of fuel-air ratios from 0.011 to 0.024.

5. At simulated sea-level takeoff conditions (589 K (600° F) inlet-air temperature and 62-N/cm^2 (90-psia) inlet total pressure) and with an average exit temperature of 1436 K (2124° F), a high smoke number level of 72 was obtained, the nitrogen oxide emission index was 4.2 grams per kilogram of fuel, the carbon monoxide emission index was 21.8 grams per kilogram of fuel, and the unburned hydrocarbon emission index was less than 0.03 gram per kilogram of fuel. At cruise conditions (890 K (1150° F) inlet-air temperature) and with an average exit temperature of 1450 K (2151° F), the smoke number level decreased to 26, the nitrogen oxide emission index increased to 12.5 grams per kilogram of fuel, the carbon monoxide emission index decreased to 5.0 grams per kilogram of fuel, and the unburned hydrocarbon emission index was less than 0.04 grams per kilogram of fuel.

6. At simulated engine idle conditions, the high combustion efficiency (near 100 percent) resulted in low emission index levels of about 28.6 for carbon monoxide and about 3.4 for unburned hydrocarbons. The emission index for oxides of nitrogen was 3.0 grams per kilogram of fuel.

7. Combustor altitude relight was obtained at an inlet pressure of 4.2 N/cm^2 (6.1 psia) with an ambient inlet-air temperature of 300 K (80° F) and a reference Mach number of 0.10. By reducing the reference Mach number to 0.05, combustor relight was

obtained at an inlet pressure of 2.8 N/cm^2 (4.1 psia) with an ambient inlet-air temperature of 294 K (70° F).

Lewis Research Center,
National Aeronautics and Space Administration,
Cleveland, Ohio, January 5, 1973,
501-24.

APPENDIX - EXHAUST EMISSION INSTRUMENTATION SYSTEM

Sampling Probes

Each gas sampling probe consisted of a common sampling tube with five sampling points located at centers of equal combustor exit area. The probes were water cooled by an adjoining U-tube, as shown in figure 24. Heating elements along the sampling line were capable of maintaining a gas sample temperature of about 450 K (350° F) at the inlet to the gas analysis system. This prevented condensation of water and minimized the adsorption and desorption effects of hydrocarbon compounds.

Gas Analysis System

The instrumentation system for gaseous emissions (fig. 25) provided for continuous analysis of carbon dioxide, carbon monoxide, oxides of nitrogen, and total hydrocarbons. The hydrocarbon content of the gas was determined by a Beckman Model 402 Hydrocarbon analyzer. This analyzer used flame ionization detection, by which hydrocarbon molecules in the exhaust sample were dissociated to form carbon ions in hydrogen flame. The hydrogen atmosphere prevented the immediate oxidation of the carbon, and the presence of polarized electrodes initiated an ionization current. This current is proportional to the carbon atoms entering the detector and is a linear measurement of the concentration of unburned hydrocarbons (assumed to be molecules of CH_2) in the sample gas.

Carbon monoxide and carbon dioxide concentrations were determined by two model 315B Beckman nondispersive infrared analyzers. The analyzers use double-beam optical paths in which the differential absorption of infrared energy is measured between a reference cell and a sample cell. The differential energy increment between cells is amplified and read as a function of the concentration of the component of interest in the sample cell. The two analyzers differed only in their appropriate cell lengths and the optical filters needed to measure the gases of interest.

Oxides of nitrogen (NO_x) were measured by a Thermo Electron Model 10A Chemiluminescent analyzer. This instrument was capable of providing separate measurements of nitric oxide (NO) and oxides of nitrogen (NO_2 + NO). The basis of detection in the analyzer is a reaction chamber where sample gas containing nitric oxide molecules mixes with ozone (O_3) molecules. A chemical reaction occurs in which excited nitrogen dioxide (NO_2) molecules are formed and emit light when they lose their excess energy. The release of light or radiation in the course of a chemical reaction is called chemiluminescence. The emitted light passes through an optical filter and is monitored by a photomultiplier. The gas sample flow is controlled such that the output from the photomultiplier is linearly proportional to the NO concentration. Oxides of nitrogen were

monitored in the same way, but the NO_2 was first converted to NO. The conversion was accomplished by passing the sample gas through a heated stainless-steel coil of sufficient temperature to reduce any NO_2 to NO.

The concentration of exhaust products in parts per million by volume (ppm) was monitored by four indicating meters, two dual-channel continuous recorders, and an on-line computer. Figure 26 is a schematic diagram of the gaseous exhaust monitoring system. The on-line computer provided a printout of emission concentrations corrected to a wet basis in terms of emission index (grams of pollutant/kilograms of fuel). Sample validity was checked by comparing the fuel-air ratio as determined by exhaust gas analysis to the fuel-air ratio as determined by separate fuel flow and airflow measurements.

Smoke Measurement System

Smoke emissions from the combustor were determined from the reflectivity of carbon stains collected on Whatman No. 4 filter paper. The schematic flow path for obtaining smoke stains is shown in figure 27. A known flow rate of 1.4×10^{-2} cubic meters per minute (0.5 ft^3/min) was passed through the smoke sampling head and allowed to stain a 3.87-square-centimeter (0.60-$in.^2$) area of the filter paper. The absolute reflectivity of the stained filter paper was measured with a Welsh Densichron using a black background. The Densichron was calibrated with a Welsh Gray Scale. The smoke number was determined from the following equation:

$$SN = 100 \times \left(1 - \frac{\text{Percent absolute reflectivity of sample}}{\text{Percent absolute reflectivity of clean paper}}\right)$$

REFERENCES

1. Roudebush, William H.: State of the Art in Short Combustors. Paper 68-22, ICAS, Sept. 1968.

2. Grobman, Jack; Jones, Robert E.; Marek, Cecil J.; and Niedzwiecki, Richard W.: Combustion. Aircraft Propulsion. NASA SP-259, 1971, pp. 97-134.

3. Humenik, Francis M.: Performance of a Short Length Turbojet Combustor Insensitive to Radial Distortion of Inlet Airflow. NASA TN D-5570, 1970.

4. Biaglow, James A.: Effect of Various Diffuser Designs on the Performance of an Experimental Turbojet Combustor Insensitive to Radial Distortion of Inlet Airflow. NASA TM X-2216, 1971.

5. Norgren, Carl T.: Design and Performance of an Experimental Annular Turbojet Combustor with High-Velocity-Air Admission Through One Wall. NASA Memo 12-28-58E, 1958.

6. Fear, James S.: Performance of a Small Annular Turbojet Combustor Designed for Low Cost. NASA TM X-2476, 1972.

7. Clarke, J. S.; and Jackson, S. R.: General Considerations in the Design of Combustion Chambers for Aircraft and Industrial Gas Turbines. Paper 444A, SAE, Jan. 1962.

8. Adam, Paul W.; and Norris, James W.: Advanced Jet Engine Combustor Test Facility. NASA TN D-6030, 1970.

9. Rusnak, J. P.; and Shadowen, J. H.: Development of an Advanced Annular Combustor. Rep. PWA-FR-2832, Pratt & Whitney Aircraft (NASA CR-72453), May 30, 1969.

10. Wear, Jerrold D.; Perkins, Porter J.; and Schultz, Donald F.: Test of a Full-Scale Annular Ram-Induction Combustor for a Mach 3 Cruise Turbojet Engine. NASA TN D-6041, 1970.

11. Glawe, George E.; Simmons, Frederick, S.; and Stickey, Truman M.: Radiation and Recovery Corrections and Time Constants of Several Chromel-Alumel Thermocouple Probes in High-Temperature, High-Velocity Gas Streams. NACA TN 3766, 1956.

12. Anon.: Aircraft Gas Turbine Engine Exhaust Smoke Measurements. Aerospace Recommended Practice 1179, SAE, May 4, 1970.

13. Grobman, Jack: Effect of Operating Variables on Pollutant Emissions from Aircraft Turbine Engine Combustors. Presented at General Motors Research Lab. Symposium, Warren, Mich., Sept. 27-28, 1971.

14. Anon.: Procedure for the Continuous Sampling and Measurement of Gaseous Emissions from Aircraft Turbine Engines. Aerospace Recommended Practice 1256, SAE, Oct. 1, 1971.

TABLE I. - OUTER-LINER DESIGN DETAILS

Liner	Item	Length		Width		Height		Flow area per individual position		Airsplit (nominal), percent	Relative flow area effectiveness coefficient
		cm	in.	cm	in.	cm	in.	cm^2	$in.^2$		
1	Primary scoop	7.62	3.00	2.95	1.16	5.71	2.25	16.84	2.61	25.0	0.85
	Primary slot, flush	6.98	2.75	2.13	.84	----	----	14.87	2.31	----	----
	Primary slot, main	6.98	2.75	2.95	1.16	----	----	20.59	3.19	----	----
	Secondary scoop	11.43	4.50	8.51	3.35	3.18	1.25	27.02	4.19	42.5	0.90
	Secondary slot 1	11.43	4.50	3.18	1.25	----	----	36.25	5.62	----	----
	Hood slot	7.62	3.00	1.27	0.50	----	----	9.68	1.50	8.4	0.50
	Secondary gap	-----	----	.64	.25	3.18	1.25	2.00	.31	3.5	1.00
	Secondary slot 2	8.89	3.50	1.27	.50	----	----	11.28	1.75	----	----
	Film cooling, primary							3.22	0.50	2.8	0.50
2	Primary scoop	3.81	1.50	2.95	1.16	4.62	1.82	13.63	2.11	25.0	0.83
	Primary slot, flush	3.18	1.25	3.18	1.25	----	----	10.05	1.56	----	----
	Primary slot, main	3.81	1.50	2.95/1.90	1.16/0.75	----	----	9.29	1.44	----	----
	Secondary scoop	11.43	4.50	5.71	2.25	3.18	1.25	18.10	2.81	35.9	0.90
	Secondary slot 1	11.43	4.50	2.54/1.90	1.0/0.75	----	----	25.38	3.94	----	----
	Secondary gap	-----	----	2.54	1.00	3.18	1.25	8.05	1.25	17.8	1.00
	Secondary slot 2	11.43	4.50	2.54	1.00	----	----	29.00	4.50	----	----
	Film cooling, primary							3.22	0.50	3.5	0.50
3	Primary scoop	3.99	1.57	3.43	1.35	4.62	1.82	15.87	2.46	30.0	0.93
	Primary slot, flush	3.00	1.18	5.08	2.00	----	----	15.22	2.36	----	----
	Primary slot, main	3.99	1.57	3.43/1.80	1.35/0.71	----	----	10.45	1.62	----	----
	Secondary scoop	11.43	4.50	7.47	2.94	3.18	1.25	23.68	3.67	----	----
	Secondary slot 1	10.16	4.00	2.21	.87	----	----	22.45	3.48	34.2	0.75
	Hood slot	7.62	3.00	1.90	.75	----	----	14.52	2.25	14.7	0.50
	Secondary slot 2	2.54/8.89	1.00/3.50	1.27/2.54	0.50/1.00	----	----	27.40	4.25	----	----
	Film cooling, primary							3.22	0.50	3.3	0.50

TABLE II. - NOMINAL TEST CONDITIONS

[Nominal inlet total pressure, PT_3, 62 N/cm^2 (90 psia); nominal airflow rate, W, 50 kg/sec (110 lb/sec).]

Test condition	Diffuser inlet Mach number M_3	Inlet total temperature TT_3		Reference velocity V_r		Combustor reference Mach number M_r
		K	^oF	m/sec	ft/sec	
Simulated takeoff	0.25	590	600	22	71	0.045
Intermediate	.28	750	900	28	91	.051
Intermediate	.30	840	1050	31	101	.054
Mach 3.0 cruise	.31	890	1150	33	108	.056

TABLE III. - COMBUSTOR OPERATING, PERFORMANCE, AND EXHAUST EMISSION DATA FOR LINER 3

(a) Operating and performance data

Run	Total pressure, PT_3		Average inlet temperature, TT_3		Airflow, W		Diffuser inlet Mach number, M_3	Reference velocity, V_r		Measured fuel-air ratio, $(f/a)_m$	Average exit temperature, TT_5		Mass-weighted average exit temperature		Pattern factor, $\bar{\delta}$	Stator factor, δ_{stator}	Rotor factor, δ_{rotor}	Combustor temperature rise, ΔT		Combustor pressure loss, $\Delta P/P$, percent	Combustion efficiency, η, percent
	N/cm^2	psia	K	°F	kg/sec	lb/sec		m/sec	ft/sec		K	°F	K	°F				K	°F		
278	61.7	89.6	591	604	49.6	109.3	0.247	21.7	71.2	------	----	----	----	----	-----	-----	-----	---	----	4.05	-----
279	61.5	89.2	581	586	49.3	108.8	.247	21.3	70.0	------	----	----	----	----	-----	-----	-----	---	----	4.23	-----
280	61.8	89.6	587	597	49.7	109.5	.246	21.6	70.9	0.0111	1000	1340	1002	1344	0.370	0.290	0.073	415	748	4.18	102.6
281	61.8	89.6	587	597	49.7	109.5	.247	21.6	70.9	.0111	1001	1342	1004	1348	.363	.283	.073	417	751	4.34	103.4
282	61.8	89.7	589	600	49.6	109.3	.246	21.6	70.9	.0129	1069	1464	1071	1469	.381	.312	.046	482	868	4.26	103.2
283	61.8	89.7	590	602	49.5	109.1	.246	21.6	70.9	.0129	1071	1468	1074	1473	.352	.284	.045	484	872	4.22	103.4
284	62.2	90.3	590	602	49.4	108.9	.244	21.4	70.3	.0147	1134	1582	1136	1586	.371	.310	.033	546	983	4.28	103.4
285	61.5	89.2	591	604	49.5	109.1	.248	21.8	71.5	.0146	1132	1578	1134	1582	.359	.297	.033	543	978	4.35	103.2
286	60.7	88.0	590	603	49.6	109.2	.252	22.0	72.4	.0165	1197	1694	1197	1695	.403	.348	.031	607	1092	4.65	103.0
287	62.0	89.9	591	604	49.4	108.9	.245	21.6	70.7	.0164	1195	1692	1196	1694	.395	.340	.032	605	1090	4.35	103.2
288	61.7	89.5	591	604	49.5	109.1	.247	21.7	71.2	.0185	1268	1822	1267	1821	.427	.378	.036	676	1216	4.43	103.4
289	61.7	89.6	591	604	49.5	109.0	.247	21.7	71.1	.0185	1264	1816	1264	1815	.423	.374	.037	673	1211	4.51	103.2
294	61.5	89.2	590	603	50.0	110.3	.250	22.0	72.1	.0200	1315	1908	1313	1904	.436	.390	.048	723	1301	4.53	103.4
295	61.6	89.3	590	603	50.0	110.2	.250	21.9	71.9	.0200	1315	1907	1313	1904	.445	.400	.047	723	1301	4.57	102.7
296	61.6	89.4	590	602	50.0	110.1	.250	21.9	71.8	.0219	1377	2019	1373	2012	.480	.437	.063	783	1409	4.60	102.8
297	61.4	89.1	590	602	49.9	110.1	.250	22.0	72.1	.0219	1375	2015	1371	2009	.479	.436	.062	781	1406	4.55	102.8
298	61.8	89.6	591	604	49.9	110.0	.248	21.8	71.7	.0228	1409	2076	1404	2068	.462	.421	.069	813	1464	4.53	102.6
299	61.9	89.7	591	605	49.9	110.0	.248	21.8	71.6	.0228	1407	2073	1403	2065	.477	.436	.068	811	1460	4.53	102.7
300	61.8	89.7	589	601	50.0	110.2	.249	21.8	71.6	.0236	1431	2116	1426	2107	.467	.427	.072	836	1505	4.56	102.9
301	61.9	89.8	589	601	49.9	110.1	.248	21.8	71.4	.0236	1430	2115	1425	2105	.484	.444	.073	836	1505	4.57	103.0
302	61.9	89.8	591	604	49.8	109.9	.248	21.8	71.4	.0148	1138	1588	1139	1591	.416	.355	.035	549	987	4.49	103.0
303	61.9	89.7	591	604	49.9	110.0	.248	21.8	71.6	------	----	----	----	----	-----	-----	-----	---	----	4.05	-----
346	61.9	89.8	588	598	50.2	110.7	.250	21.8	71.5	------	----	----	----	----	-----	-----	-----	---	----	4.05	-----
347	62.0	89.9	586	595	49.3	108.8	.245	21.3	69.9	------	----	----	----	----	-----	-----	-----	---	----	4.15	-----
348	62.3	90.3	591	604	49.1	108.2	.243	21.3	69.8	.0149	1143	1597	1144	1600	.464	.404	.034	554	997	4.14	103.9
349	62.2	90.2	592	605	49.0	108.1	.244	21.3	70.0	.0185	1271	1828	1270	1827	.471	.422	.028	679	1222	4.15	104.1
350	62.9	91.2	592	606	48.9	107.9	.240	21.1	69.1	.0223	1395	2052	1392	2046	.416	.374	.046	800	1440	4.25	103.9
351	62.1	90.1	593	607	49.1	108.3	.245	21.4	70.3	------	----	----	----	----	-----	-----	-----	---	----	3.85	-----
353	61.7	89.5	593	608	49.0	108.0	.245	21.5	70.6	------	----	----	----	----	-----	-----	-----	---	----	3.93	-----
354	62.0	90.0	595	611	48.9	107.8	.244	21.4	70.4	.0168	1212	1722	1213	1725	.383	.329	.036	619	1114	4.22	104.1
355	62.3	90.4	595	612	48.9	107.7	.243	21.3	70.0	.0205	1341	1955	1341	1953	.403	.359	.029	745	1342	4.34	104.6
356	62.0	89.9	594	609	49.0	108.0	.245	21.5	70.5	.0223	1399	2059	1397	2056	.429	.387	.039	804	1446	4.32	104.4
357	61.8	89.6	595	612	49.0	108.1	.246	21.6	70.9	.0235	1438	2129	1436	2124	.437	.397	.045	840	1512	4.29	104.2
358	62.3	90.3	768	922	48.5	106.8	.279	27.3	89.5	.0115	1175	1656	1179	1663	.372	.326	.093	411	741	5.17	102.9
359	62.2	90.2	765	918	48.6	107.2	.280	27.3	89.7	.0123	1201	1702	1205	1709	.339	.328	.082	440	791	5.21	102.9
360	63.0	91.4	764	915	48.3	106.4	.273	26.7	87.6	.0142	1265	1817	1269	1824	.320	.307	.064	505	909	5.00	103.4
361	62.3	90.3	765	918	48.6	107.1	.279	27.3	89.5	.0164	1341	1954	1344	1960	.307	.302	.045	579	1042	5.28	103.5
362	62.1	90.0	764	916	48.5	107.0	.279	27.3	89.5	.0183	1403	2066	1406	2071	.274	.270	.033	642	1156	5.22	104.0
363	62.3	90.3	765	917	48.5	106.8	.278	27.2	89.1	.0202	1466	2178	1467	2182	.305	.264	.029	703	1265	5.26	104.1
364	61.6	89.3	765	917	48.3	106.6	.281	27.4	89.9	.0208	1486	2214	1487	2217	.319	.273	.028	722	1300	5.49	104.1
365	62.0	90.0	765	918	48.6	107.3	.280	27.4	89.9	.0206	1481	2205	1483	2209	.325	.278	.028	717	1291	5.35	104.2
366	61.9	89.7	843	1059	48.5	107.0	.298	30.2	99.1	.0192	1333	1940	1338	1948	.343	.285	.075	494	889	5.81	103.1
367	62.4	90.5	844	1059	48.4	106.7	.294	29.9	98.0	.0164	1409	2077	1413	2085	.318	.276	.054	570	1025	5.76	103.6
368	62.1	90.1	843	1058	48.4	106.7	.295	30.0	98.4	.0174	1441	2133	1445	2141	.319	.280	.050	601	1082	5.85	103.6
369	62.8	91.1	846	1062	48.1	106.1	.290	29.6	97.1	.0189	1488	2219	1492	2227	.341	.298	.040	647	1164	5.60	103.7
371	62.2	90.3	896	1153	48.2	106.2	.304	31.7	103.9	.0135	1359	1986	1364	1995	.320	.307	.088	467	841	6.00	103.6
372	61.5	89.3	897	1156	48.4	106.7	.310	32.2	105.7	.0151	1412	2082	1417	2092	.335	.290	.080	520	936	6.15	103.6
373	62.0	90.0	896	1154	48.3	106.4	.306	31.8	104.4	.0161	1445	2141	1450	2151	.294	.289	.071	554	996	6.05	103.7
374	41.6	60.3	843	1058	32.9	72.5	.300	30.4	99.8	------	----	----	----	----	-----	-----	-----	---	----	5.67	-----
375	62.3	90.3	898	1157	49.1	108.4	.311	32.3	106.0	-----	----	----	----	----	-----	-----	-----	---	----	5.86	-----
376	62.1	90.1	848	1067	48.5	107.0	.297	30.2	99.2	-----	----	----	----	----	-----	-----	-----	---	----	5.35	-----
377	63.0	91.3	772	929	49.0	108.1	.280	27.4	90.1	-----	----	----	----	----	-----	-----	-----	---	----	4.87	-----
378	62.3	90.4	547	524	49.3	108.6	.233	19.8	64.9	-----	----	----	----	----	-----	-----	-----	---	----	3.32	-----

TABLE III. - Concluded. COMBUSTOR OPERATING, PERFORMANCE, AND EXHAUST EMISSION DATA FOR LINER 3

(b) Exhaust emissions data

Run	Oxides of nitrogen, $NO_x = NO + NO_2$		Nitric oxide, NO		Ratio of nitric oxides to oxides of nitrogen, NO/NO_x, percent	Unburned hydrocarbons, HC		Carbon monoxide, CO		Carbon dioxide, CO_2		Gas sample fuel-air ratio, $(f/a)_{gs}$	Ratio of gas sample to measured fuel-air ratio, $\frac{(f/a)_{gs}}{(f/a)_m}$	Smoke number, SN
	ppm	$\frac{g(NO_2)}{kg\ fuel}$	ppm	$\frac{g(NO_2)}{kg\ fuel}$		ppm	$\frac{g(CH_2)}{kg\ fuel}$	ppm	$\frac{g(CO)}{kg\ fuel}$	ppm	$\frac{g(CO_2)}{kg\ fuel}$			
281	34.0	4.91	27.0	3.90	79.4	<1.0	<0.044	87.6	7.70	15 540	2147	0.0077	69.2	21.2
282	38.9	4.84	31.0	3.86	79.7		<.038	116.4	8.82	18 332	2201	.0090	70.0	37.0
283	39.7	4.94	31.5	3.92	79.3		<.038	118.9	9.01	18 210	2186	.0090	69.5	----
284	45.8	5.01	36.0	3.94	78.6		<.033	171.2	11.41	20 308	2141	.0100	68.4	49.5
285	45.2	4.98	36.5	4.02	80.7		<.033	170.3	11.42	19 808	2103	.0097	67.0	----
287	51.2	5.03	40.0	3.93	78.1		<.030	253.4	15.16	22 306	2110	.0114	67.2	55.5
288	55.9	4.88	46.5	4.06	83.2		<.027	370.0	19.67	24 303	2152	.0108	65.6	57.7
289	57.7	5.04	48.0	4.19	83.2		<.027	370.2	19.68	24 077	2068	.0120	65.1	----
294	62.5	5.06	----	----	----		<.025	450.7	22.19	28 910	2259	.0148	72.4	----
295	63.0	5.10	55.0	4.45	87.3		<.025	459.1	22.61	28 760	2247	.0142	72.1	63.7
296	70.3	5.20	62.0	4.59	88.2		<.022	562.9	25.36	31 624	2259	.0159	72.7	68.0
297	70.2	5.19	62.5	4.62	89.0		<.022	600.7	27.06	31 226	2241	.0158	71.9	----
298	74.2	5.28	67.0	4.77	90.3		<.022	628.1	27.20	31 929	2192	.0161	70.5	66.3
299	74.5	5.30	----	----	----		<.022	632.1	27.38	32 358	2221	.0163	71.5	----
300	77.1	5.30	70.0	4.81	90.8		<.021	694.9	29.10	33 294	2209	.0167	71.1	68.5
301	76.1	5.23	----	----	----		<.021	674.7	28.25	32 590	2163	.0164	69.6	----
354	46.0	4.47	43.5	4.23	94.6		<.029	200.3	11.86	26 361	2452	.0129	78.0	59.0
355	54.9	4.38	52.5	4.19	95.6		<.024	344.7	16.75	31 001	2368	.0152	75.5	69.6
356	57.5	4.22	54.5	4.00	94.8		<.022	467.3	20.88	34 908	2451	.0175	78.4	72.5
357	59.7	4.16	56.5	3.94	94.6		<.022	512.9	21.77	35 162	2345	.0176	74.8	----
358	62.0	8.77	53.5	7.57	86.3		<.042	46.8	4.03	19 202	2597	.0095	82.3	27.5
359	63.6	8.42	54.0	7.15	84.9		<.040	55.0	4.41	21 435	2706	.0106	85.8	29.0
360	67.1	7.70	58.0	6.66	86.4		<.034	80.0	5.58	24 658	2705	.0122	85.8	32.8
361	76.2	7.56	66.5	6.60	87.3		<.030	126.6	7.65	27 619	2621	.0136	83.2	39.4
362	85.7	7.65	75.0	6.69	87.5		<.027	179.4	9.75	31 006	2647	.0154	84.1	46.1
363	95.6	7.75	81.5	6.61	85.2		<.024	239.7	11.83	34 939	2710	.0172	86.2	55.0
364	100.4	7.90	89.0	7.00	88.6		<.024	276.3	13.24	35 369	2664	.0170	84.8	57.0
365	96.8	7.69	----	----	----		<.024	251.3	12.15	36 013	2736	.0175	87.1	----
366	88.6	10.16	77.5	8.89	87.5		<.034	64.2	4.48	23 943	2627	.0124	87.6	32.0
367	103.2	10.23	91.5	9.07	88.7		<.030	94.1	5.68	28 319	2686	.0140	85.2	37.2
368	107.9	10.09	97.5	9.12	90.4		<.028	116.6	6.64	29 844	2670	.0147	84.7	42.2
369	120.2	10.41	102.5	8.88	85.3		<.026	145.9	7.69	32 478	2689	.0161	85.3	47.4
371	110.1	13.27	97.5	11.75	88.6		<.036	45.4	3.34	24 269	2798	.0120	88.7	27.0
372	114.2	12.30	102.0	11.00	89.3		<.032	66.4	4.96	26 796	2762	.0132	87.5	26.4
373	123.4	12.47	108.2	10.93	87.7		<.030	80.0	4.94	29 378	2839	.0145	90.0	26.4

TABLE IV. - COMBUSTOR IDLE DATA FOR LINER 2

(a) Operating and performance data

Run	Total pressure, PT_3		Average inlet temperature, TT_3		Airflow, W		Diffuser inlet Mach number, M_3	Reference velocity, V_r		Measured fuel-air ratio, $(f/a)_m$	Arithmetic average exit temperature, TT_5		Mass-weighted average exit temperature		Combustor temperature rise, ΔT		Combustor pressure loss, $\Delta P/P$, percent	Combustion efficiency, η, percent	Fuel nozzle differential pressure	
	N/cm^2	psia	K	^oF	kg/sec	lb/sec		m/sec	ft/sec		K	^oF	K	^oF	K	^oF			N/cm^2	psid
226	40.8	59.2	473	392	36.3	80.1	0.245	19.3	63.3	0.0125	959	1266	953	1256	480	864	4.77	102.5	58	85
227	41.8	60.6	476	397	37.2	82.0	.245	19.4	63.6	.0099	857	1084	854	1078	378	681	4.84	100.4	39	57
228	41.4	60.0	480	405	37.1	81.9	.249	19.7	64.7	.0075	770	926	768	921	287	517	4.90	98.7	23	34

(b) Exhaust emission data

Run	Oxides of nitrogen, NO_x		Nitric oxide, NO		Ratio of nitric oxides to oxides of nitrogen, NO/NO_x, percent	Unburned hydrocarbons, HC		Carbon monoxide, CO		Carbon dioxide, CO_2		Gas sample fuel-air ratio, $(f/a)_{gs}$	Ratio of gas sample to measured fuel-air ratio, $\frac{(f/a)_{gs}}{(f/a)_m}$
	ppm	$\frac{g(NO_2)}{kg\ fuel}$	ppm	$\frac{g(NO)}{kg\ fuel}$		ppm	$\frac{g(CH_2)}{kg\ fuel}$	ppm	$\frac{g(CO)}{kg\ fuel}$	ppm	$\frac{g(CO_2)}{kg\ fuel}$		
226	18.3	2.37	13	1.69	71.1	35.9	1.41	289	22.7	17 648	2186	0.0088	70.4
227	14.3	2.37	10	1.66	70.0	46.8	2.35	253	25.4	13 486	2130	.0067	68.2
228	13.9	3.00	9	1.91	64.6	56.6	3.72	227	29.8	11 938	2465	.0060	79.6

TABLE V. - ALTITUDE RELIGHT DATA

(a) Ignition points at altitude relight conditions - liners 1 and 2

Run	Liner	Total pressure, PT_3		Average inlet temperature, TT3		Airflow, W		Diffuser inlet Mach number, M_3	Combustor reference Mach number, M'_r	Reference velocity, V_r		Fuel-air ratio, f/a	Arithmetical average exit temperature		Mass-average exit temperature		Combustor temperature rise, ΔT		Combustor pressure loss, $\Delta P/P$	Combustion efficiency, η, percent	Fuel nozzle differential pressure	
		N/cm^2	psia	K	^oF	kg/sec	lb/sec			m/sec	ft/sec		K	^oF	K	^oF	K	^oF			N/cm^2	psid
112	1	10.9	15.8	296	73	19.7	43.4	0.415	0.097	23.8	78.2	0.006	---	----	---	----	---	----	-----	----	---	---
122		6.6	9.6	291	65	12.9	28.5	.457	.105	25.8	84.5	.0144	---	----	---	----	---	----	-----	----	---	---
125		6.0	8.7	286	56	8.8	19.5	.318	.080	19.2	63.1	.0139	---	----	---	----	---	----	-----	----	---	---
136		5.4	7.8	286	56	6.3	13.8	.243	.063	15.3	50.1	.0157	---	----	---	----	---	----	-----	----	---	---
157		5.4	7.9	425	306	8.3	18.2	.409	.098	29.1	95.4	.0171	---	----	---	----	---	----	-----	----	---	---
164		5.4	7.8	420	297	7.3	16.2	.366	.090	26.4	86.5	.0168	---	----	---	----	---	----	-----	----	---	---
232	2	9.0	13.0	301	82	16.0	35.3	.416	.099	24.3	79.6	.0078	502	444	499	439	198	356	12.86	61.9	213	310
251		4.1	6.0	298	78	7.4	16.4	.418	.099	24.4	79.9	.0152	525	485	524	483	225	405	14.77	38.2	180	261
254		2.8	4.1	294	70	3.0	6.6	.229	.057	14.2	46.5	.0221	737	867	743	878	449	809	-----	54.8	60	87
261		3.5	5.1	289	61	3.4	7.6	.206	.053	13.1	42.9	.0232	998	1336	992	1326	703	1266	3.86	82.3	88	128

TABLE V. - Concluded. ALTITUDE RELIGHT DATA

(b) Altitude relight performance - liner 2

Run	Total pressure, PT_3		Average inlet temperature, TT_3		Airflow, W		Diffuser inlet Mach number, M_3	Combustor reference Mach number, M'_r	Reference velocity, V_r		Fuel-air ratio, f/a	Arithmetical average exit temperature		Mass-average exit temperature		Combustor temperature rise, ΔT		Combustor pressure loss, $\Delta P/P$, percent	Combustion efficiency, η, percent	Fuel nozzle differential pressure	
	N/cm^2	psia	K	°F	kg/sec	lb/sec			m/sec	ft/sec		K	°F	K	°F	K	°F			N/cm^2	psid
231	8.8	12.8	301	82	15.7	34.5	0.416	0.099	24.2	79.3	------	----	----	----	----	---	----	12.19	----	---	---
234	9.3	13.4	301	83	15.8	34.8	.395	.095	23.3	76.5	0.0101	651	711	646	703	345	620	12.05	85.6	353	511
235	9.0	13.1	301	83	15.7	34.6	.406	.097	23.8	78.2	.0124	700	801	695	791	393	708	12.84	80.5	539	782
236	9.0	13.1	301	83	15.8	34.7	.406	.097	23.8	78.1	.0124	701	802	695	792	394	709	12.82	80.9	539	782
237	9.0	13.1	301	83	15.8	34.8	.408	.098	23.9	78.5	.0112	677	759	672	750	370	667	12.95	83.5	440	638
238	8.8	12.8	302	83	15.7	34.7	.420	.099	24.4	79.9	.0093	589	601	585	594	284	511	13.53	75.8	302	438
239	8.3	12.0	302	83	14.7	32.4	.419	.099	24.3	79.9	.0099	606	631	602	623	300	540	13.69	75.3	301	436
240	6.9	10.0	302	83	12.4	27.4	.425	.101	24.6	80.7	.0118	641	694	636	685	334	602	14.26	72.0	302	438
241	5.5	8.0	301	83	10.1	22.3	.433	.102	25.0	81.9	.0144	553	537	551	532	249	449	14.82	44.5	301	436
242	5.5	8.0	301	83	10.1	22.3	.433	.102	25.0	81.9	.0145	556	541	553	536	252	454	14.58	44.9	301	437
243	4.9	7.0	301	82	8.8	19.4	.431	.101	24.7	81.1	.0166	467	382	466	380	165	298	13.39	26.1	302	438
244	4.2	6.1	301	81	7.5	16.6	.424	.099	24.4	80.1	.0193	405	269	405	269	104	187	14.34	14.3	300	435
245	4.2	6.1	300	81	7.6	16.7	.429	.101	24.6	80.8	.0208	390	243	390	243	90	162	14.41	11.5	356	516
246	4.2	6.1	300	80	7.6	16.7	.424	.101	24.5	80.4	.0178	433	319	432	318	132	238	14.08	19.5	256	371
247	4.2	6.2	300	80	7.6	16.7	.419	.099	24.2	79.3	.0167	495	431	494	429	194	349	14.33	30.3	226	327
248	4.3	6.2	299	79	7.6	16.7	.417	.098	24.1	78.9	.0147	545	521	544	519	244	439	14.27	43.0	173	251
249	3.8	5.5	299	79	6.1	13.5	.371	.090	22.0	72.3	.0182	582	589	581	585	281	506	12.02	40.8	174	253
250	4.1	6.0	299	78	7.4	16.2	.413	.098	24.1	79.0	------	----	----	----	----	---	----	13.04	----	---	---
252	2.9	4.2	296	72	5.1	11.3	.425	.098	23.8	78.0	------	----	----	----	----	---	----	10.53	----	---	---
253	3.7	5.3	295	72	4.4	9.7	.269	.066	16.1	52.8	------	----	----	----	----	---	----	4.57	----	---	---
255	3.2	4.6	294	69	2.9	6.4	.222	.050	12.1	39.8	.0198	525	486	522	481	229	412	-----	30.7	45	65
256	3.0	4.3	294	69	2.9	6.4	.222	.053	12.9	42.5	.0273	909	1175	901	1162	607	1093	-----	61.8	87	127
257	3.4	4.9	293	68	2.9	6.5	.225	.048	11.3	37.0	.0312	912	1181	896	1154	603	1085	-----	54.7	117	170
258	2.8	4.1	293	68	4.9	10.7	.390	.097	22.7	74.4	.0187	438	329	423	303	131	235	11.82	18.4	116	168
259	3.5	5.1	293	67	4.9	10.8	.400	.076	17.8	58.6	.0232	359	187	358	185	66	118	8.34	7.7	182	264
260	3.6	5.3	292	67	2.9	6.4	.222	.043	10.3	33.9	------	----	----	----	----	---	----	3.71	----	42	62
262	3.5	5.1	289	61	3.4	7.5	.203	.053	12.9	42.3	.0201	877	1120	874	1113	585	1053	3.27	77.7	65	95
263	3.5	5.1	289	60	3.4	7.6	.207	.053	13.1	43.0	.0264	1011	1360	1003	1347	715	1287	3.73	74.8	116	168
264	3.5	5.1	288	60	6.2	13.6	.395	.095	23.0	75.5	.0148	474	395	473	392	184	332	12.23	32.1	115	167
265	3.4	5.0	288	59	6.2	13.6	.405	.098	23.4	76.9	.0165	468	383	468	382	180	323	12.84	28.3	146	212
266	4.7	6.9	288	58	8.6	19.1	.417	.099	23.9	78.3	.0157	497	435	493	428	206	370	13.74	34.0	261	378
267	4.7	6.8	288	58	8.7	19.1	.425	.101	24.2	79.4	.0170	425	305	423	301	135	243	13.82	20.7	311	451
268	4.8	7.0	287	58	8.7	19.1	.408	.098	23.4	76.9	.0145	555	540	551	532	264	474	13.32	46.7	224	325
270	4.8	7.0	287	57	8.7	19.2	.409	.098	23.5	77.1	.0132	561	550	559	546	271	489	13.23	52.3	186	270
271	4.8	7.0	287	57	8.7	19.2	.407	.098	23.4	76.9	.0144	562	552	558	545	271	488	13.04	48.2	224	324
272	4.7	6.8	287	57	8.7	19.2	.421	.101	24.0	78.7	.0118	470	386	469	385	182	328	13.62	39.0	150	217
273	5.5	8.0	287	57	9.9	21.8	.409	.098	23.4	76.7	.0116	529	493	527	489	240	432	13.15	52.1	184	268
274	5.6	8.1	287	57	9.9	21.8	.396	.095	22.9	75.2	.0127	615	648	611	641	324	584	12.57	64.9	222	322
275	5.6	8.2	287	57	9.9	21.8	.395	.095	22.8	74.9	.0138	629	672	621	659	334	602	12.56	61.9	266	386
276	5.5	8.0	287	56	9.9	21.8	.406	.098	23.3	76.4	.0150	537	507	532	497	245	441	13.04	42.1	313	454
277	5.6	8.1	287	56	9.9	21.8	.400	.097	23.0	75.6	------	----	----	----	----	---	----	11.77	----	---	---

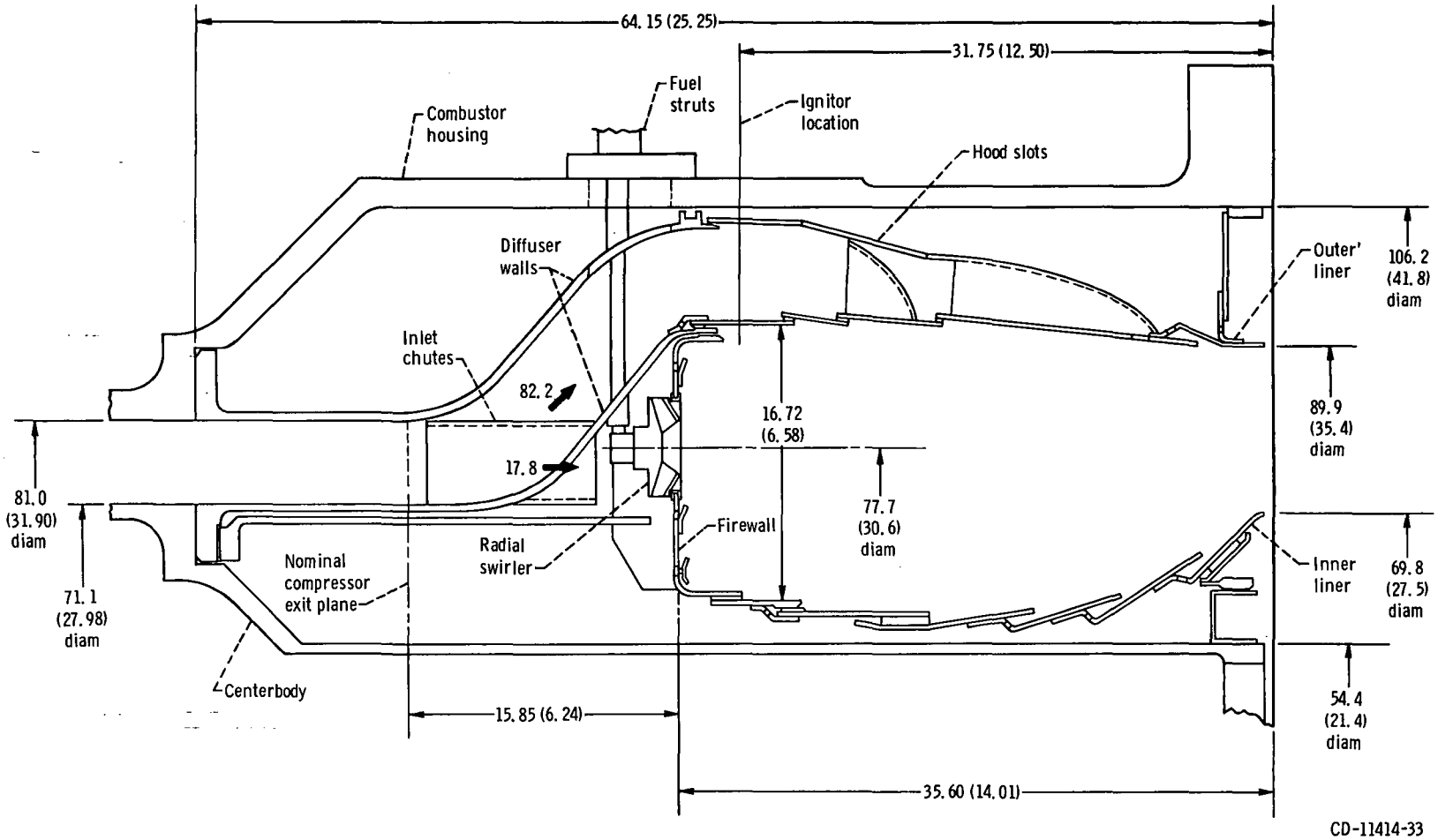

Figure 1. - Cross-sectional sketch of side-entry combustor. Dimensions are in cm (in.).

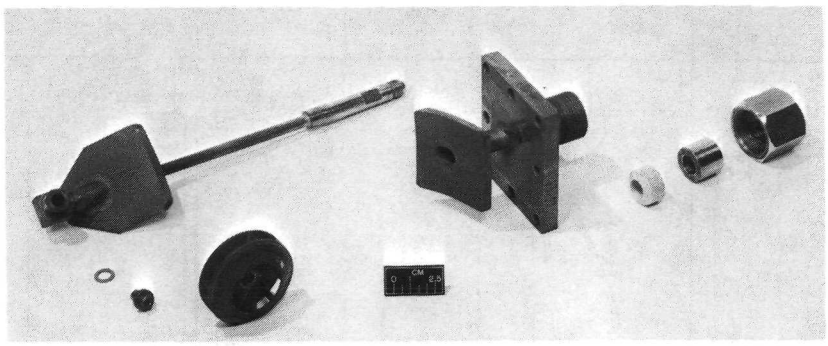

C-72-2905

Figure 2. - Fuel strut parts with radial swirler.

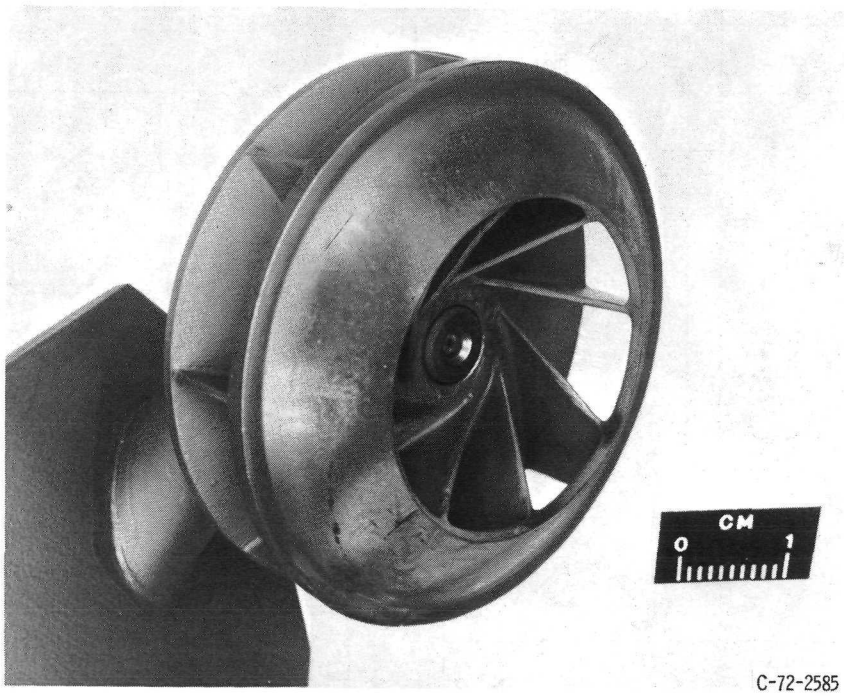

C-72-2585

Figure 3. - Final assembly with radial swirler.

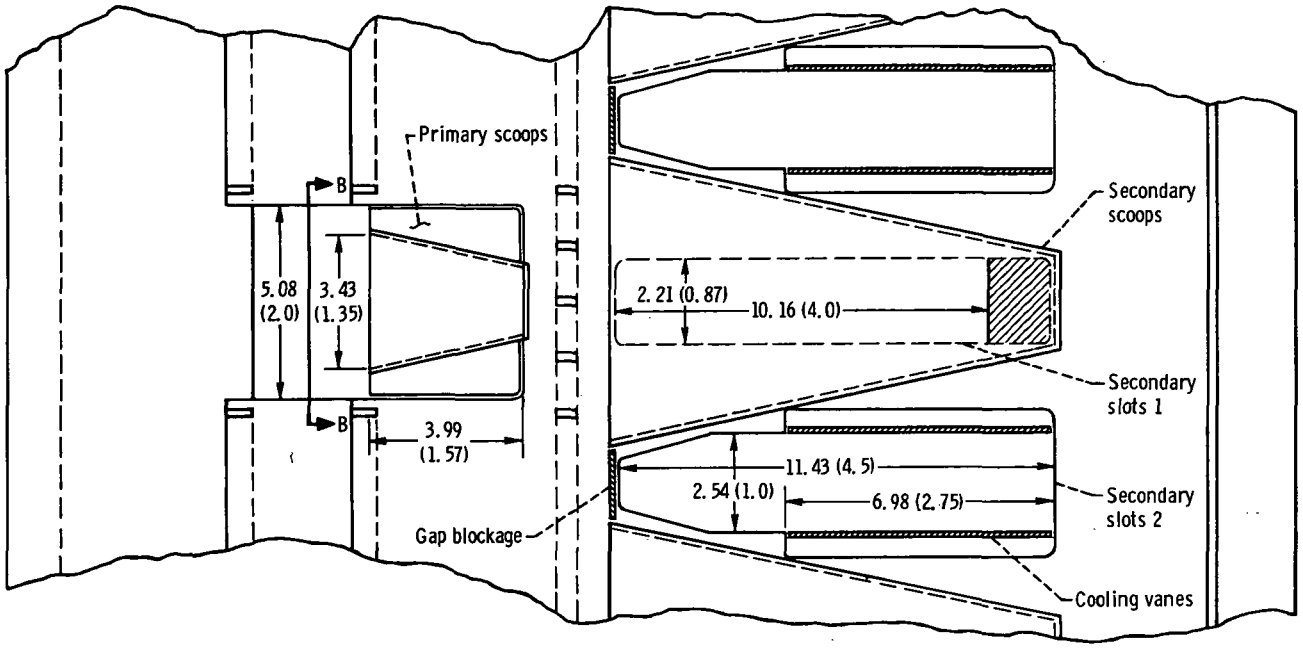

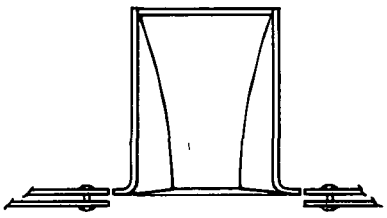

(a) Top view without hood.

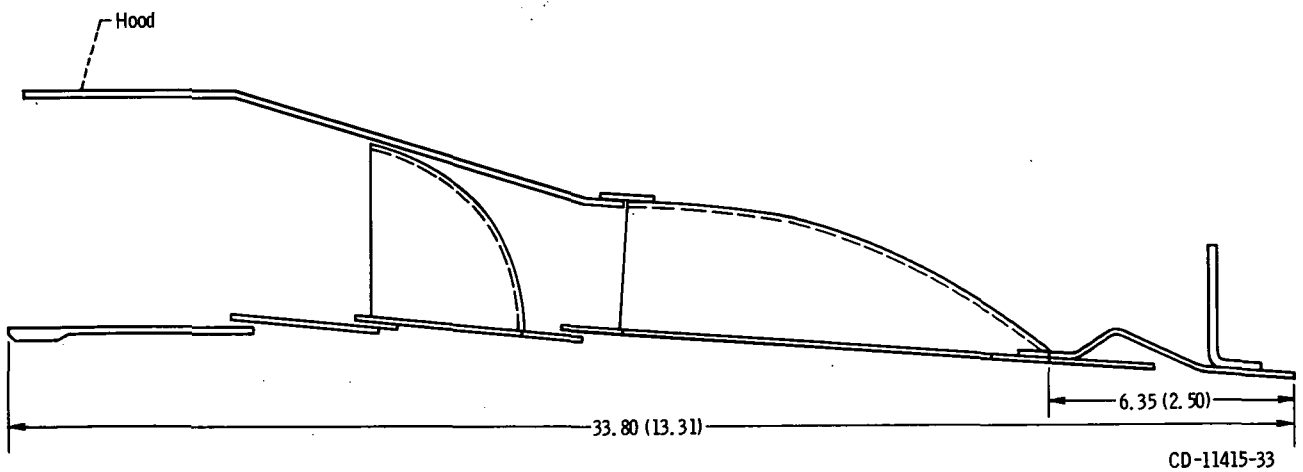

(b) Side view.

Figure 4. - Slot and scoop arrangement for outer liner 3. Dimensions are in cm (in.). For other design details, see table I.

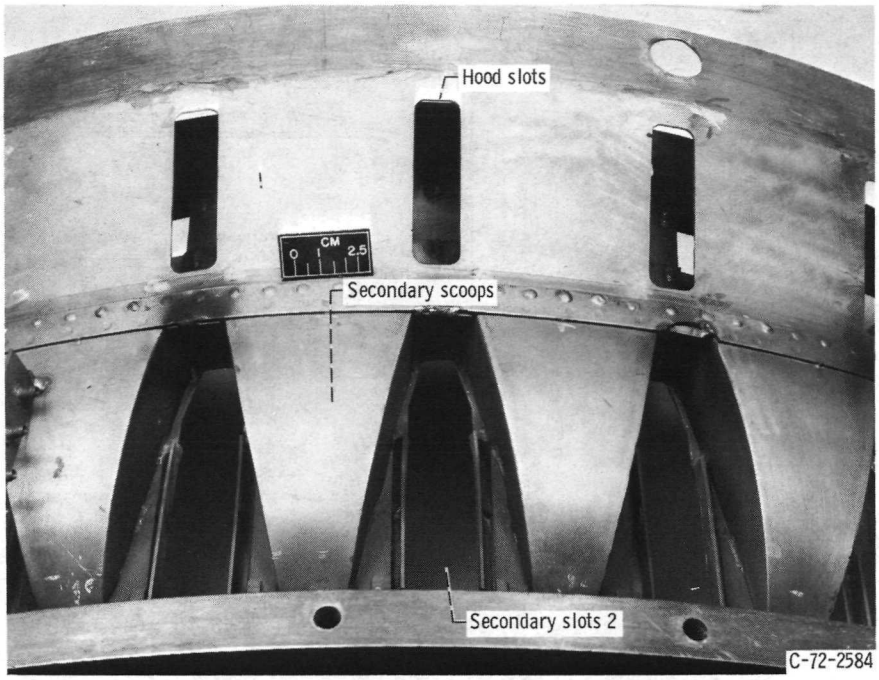

Figure 5. - Top view of liner 3, showing hood slot arrangement.

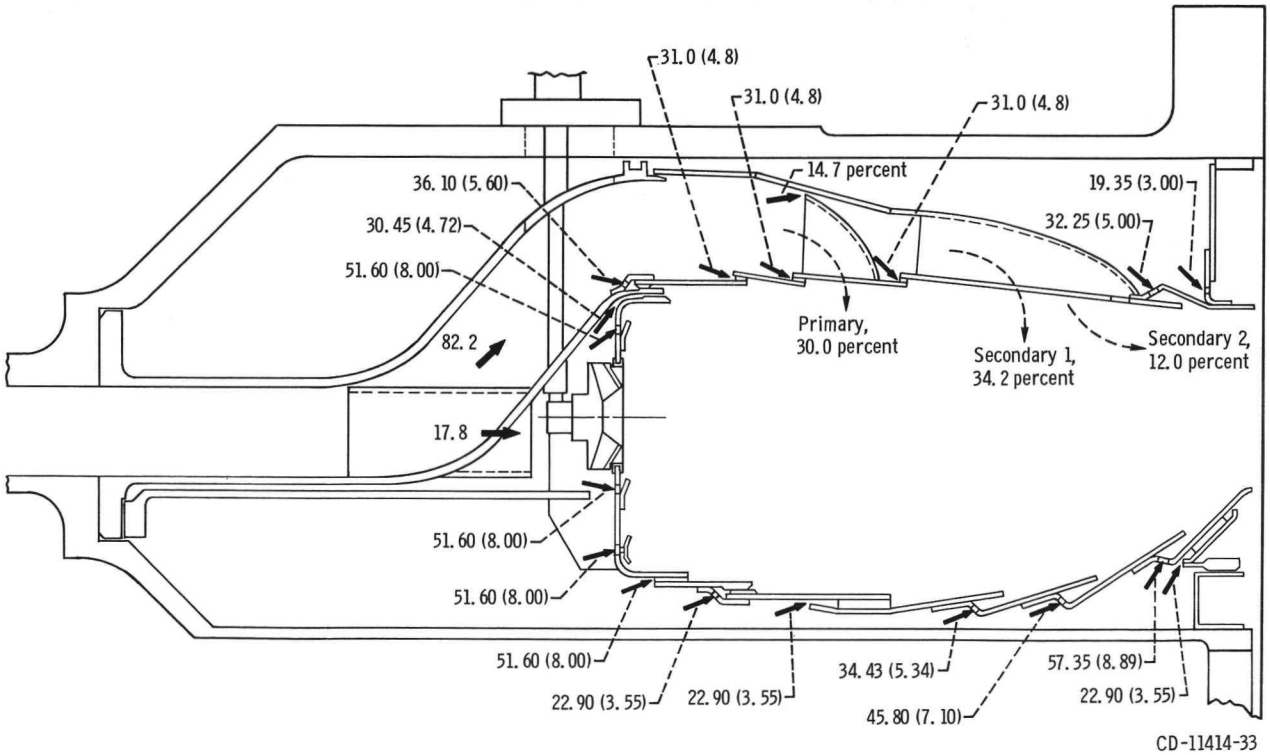

Figure 6. - Side-entry combustor airflow distribution with outer liner 3. Flow areas are in cm^2 ($in.^2$).

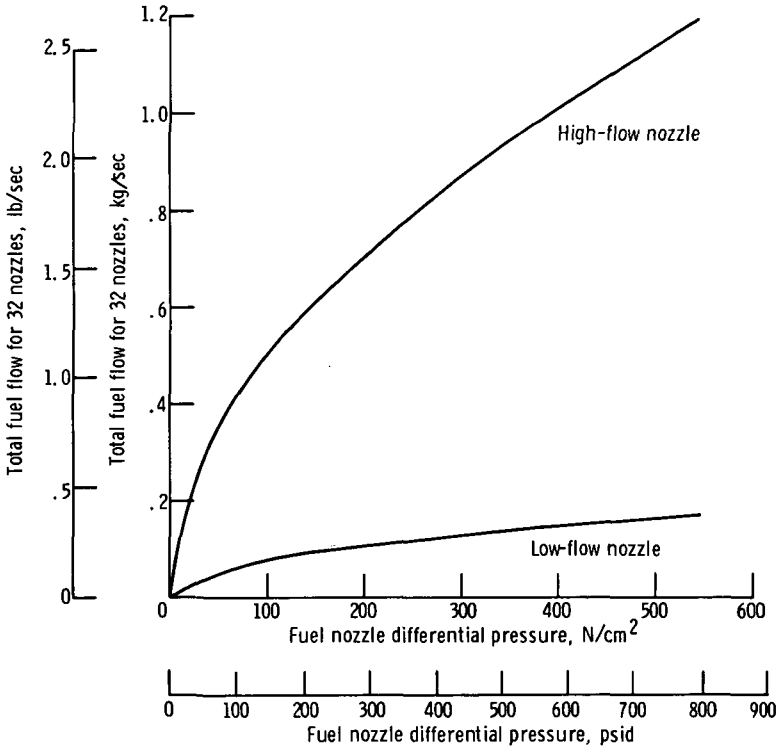

Figure 7. - Flow characteristics of fuel nozzles.

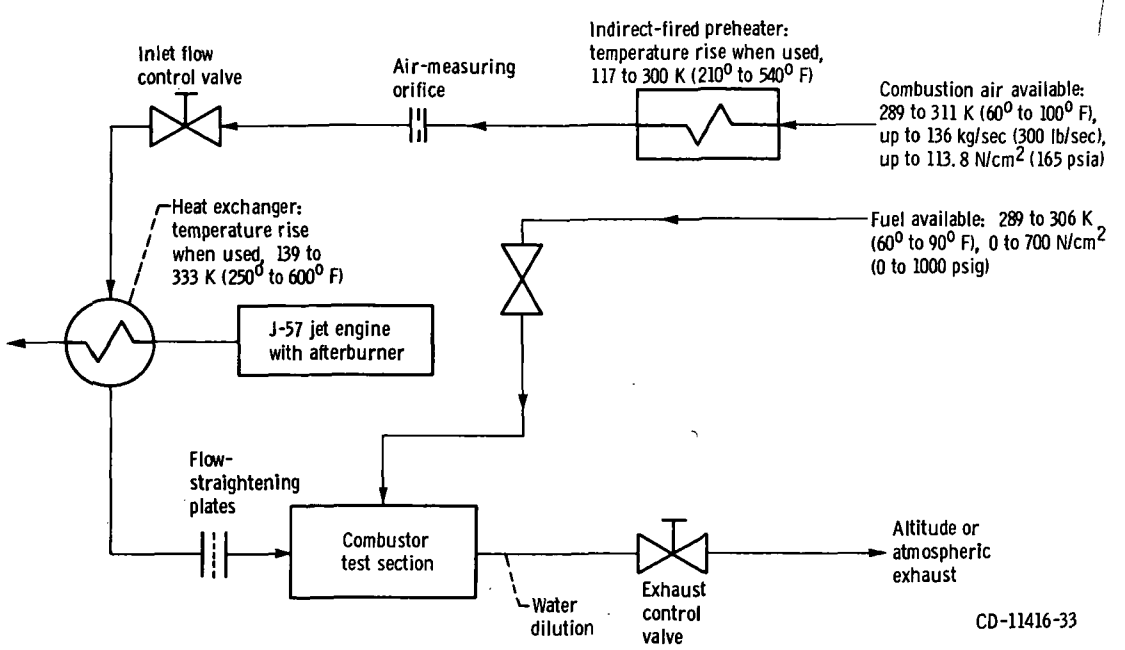

(a) Schematic of combustion air and fuel flow.

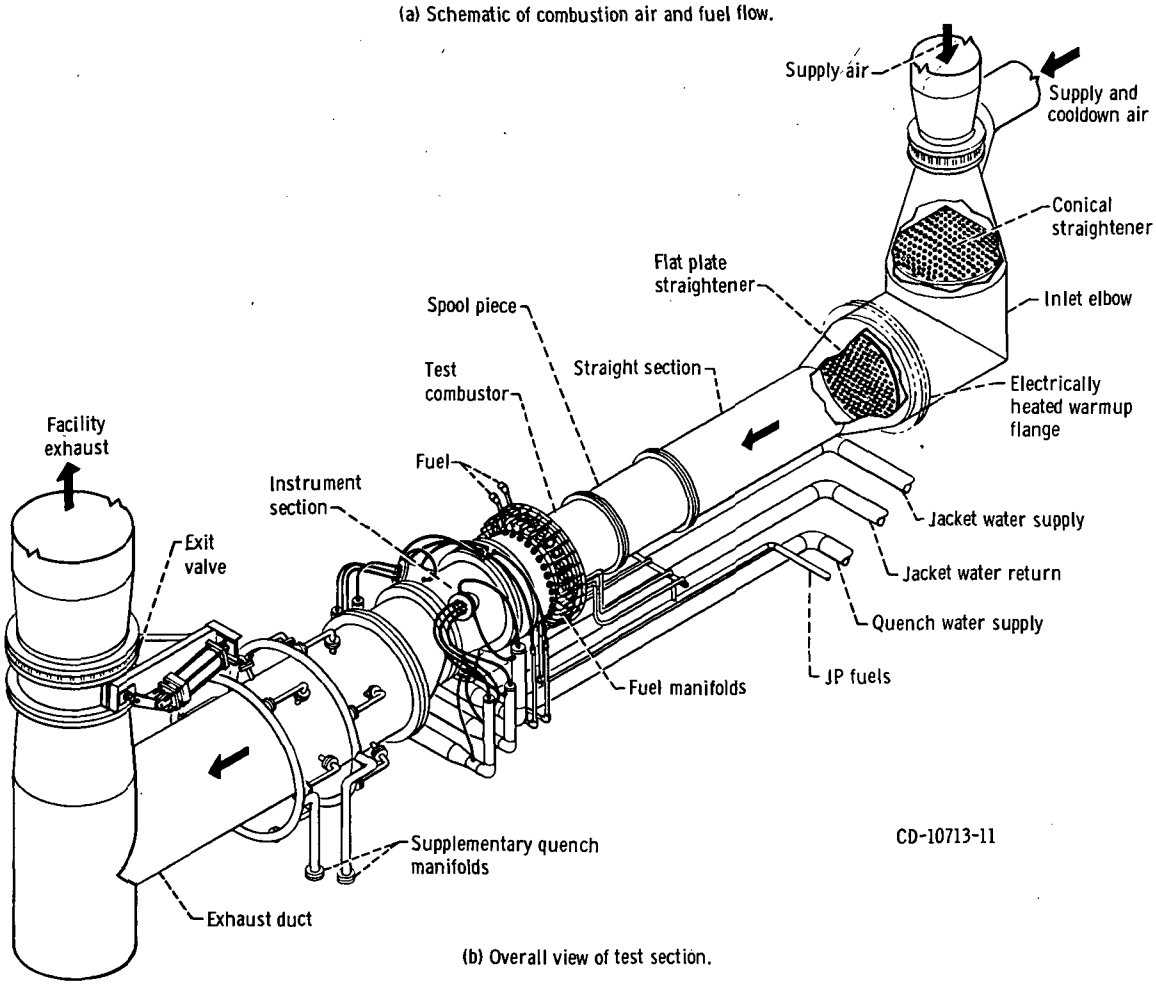

(b) Overall view of test section.

Figure 8. - Connected-duct test facility.

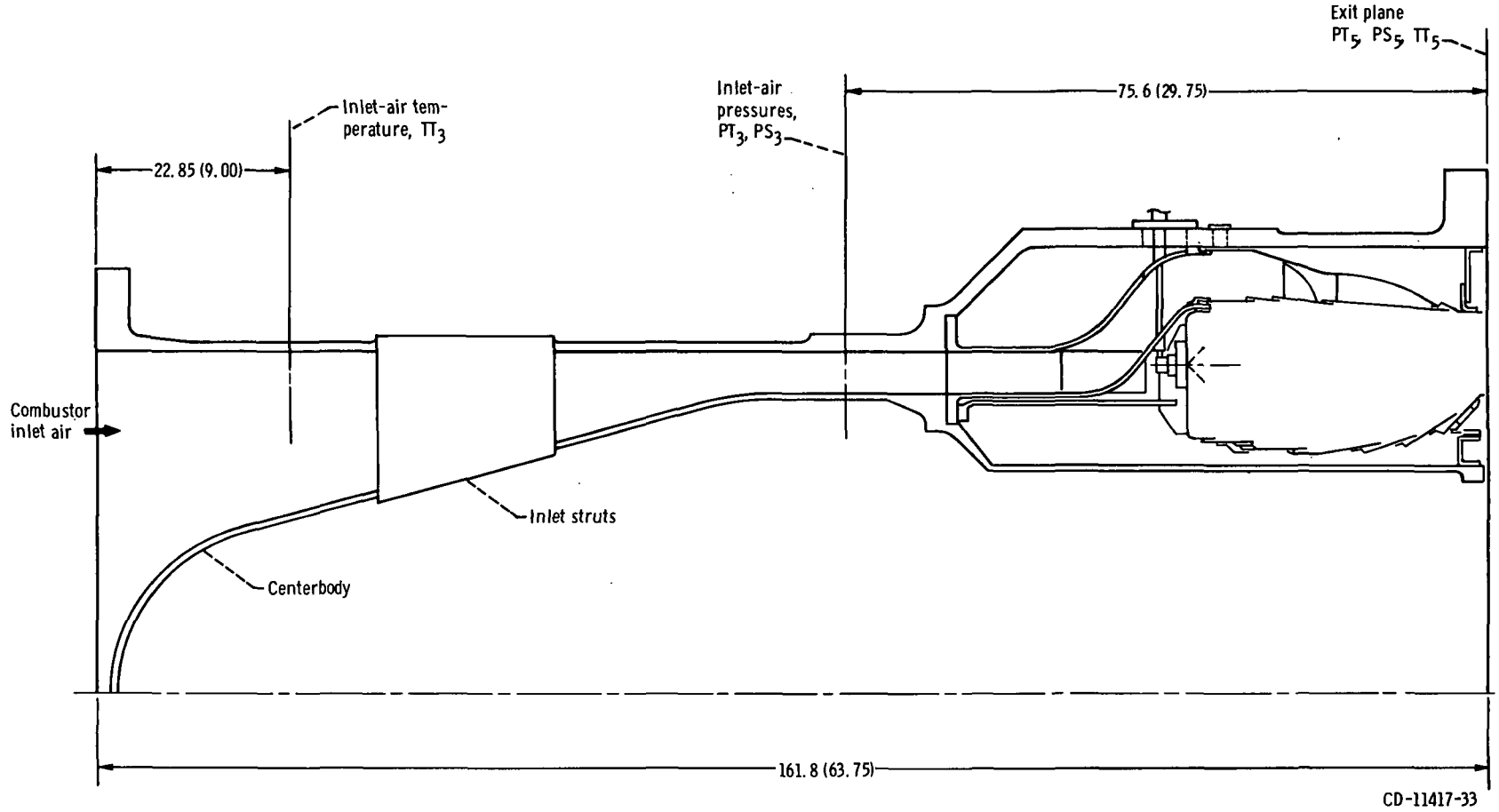

Figure 9. - Combustor housing and test section, showing axial locations of instrumentation. Dimensions are in cm (in.).

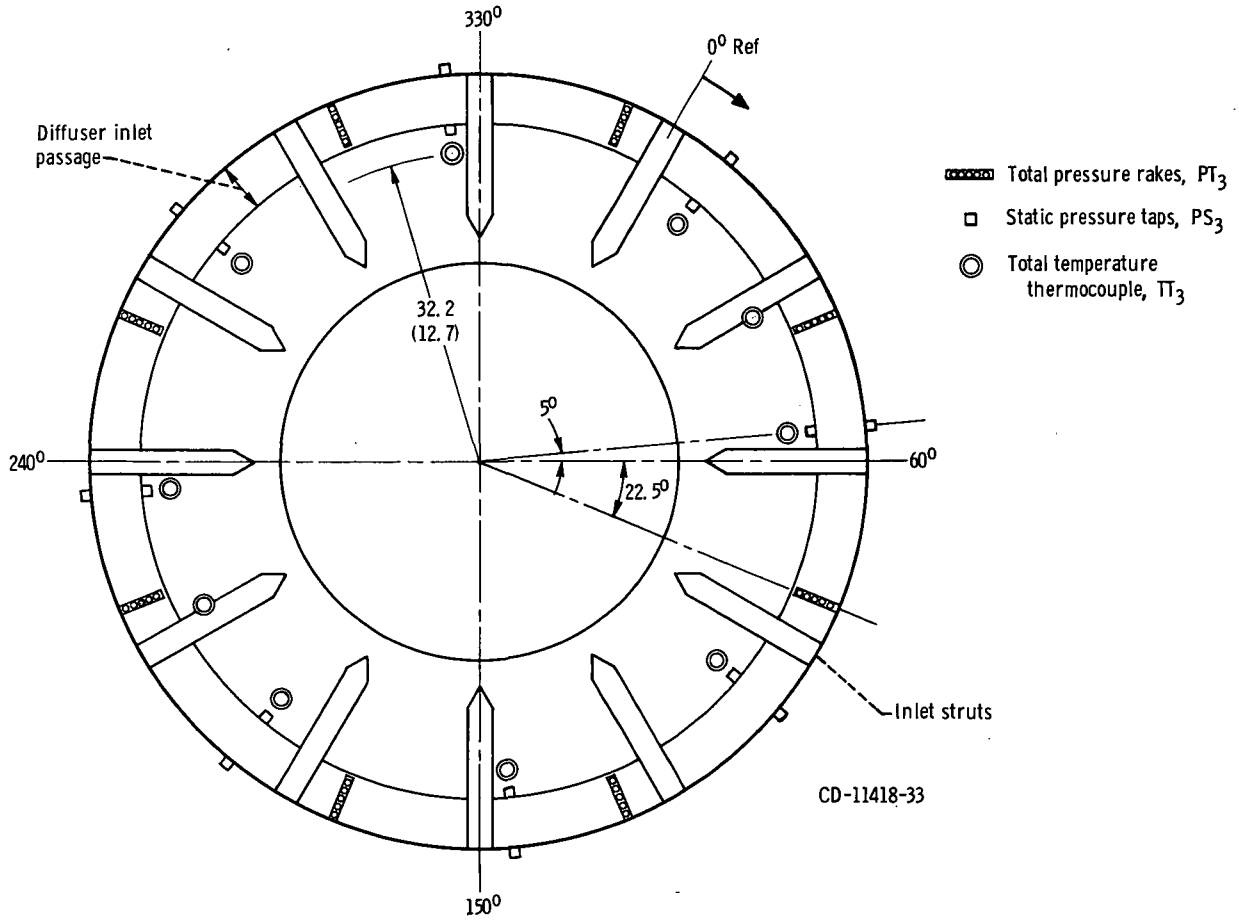

Figure 10. - Location of combustor inlet instrumentation. View looking downstream. Dimensions are in cm (in.).

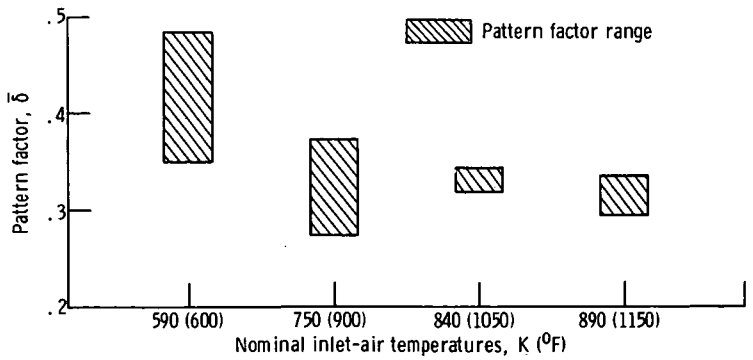

Figure 11. - Range of pattern factor variation with nominal test conditions corresponding to inlet-air pressure of 62 N/cm^2 (90 psia) and fuel-air ratios from 0.011 to 0.024.

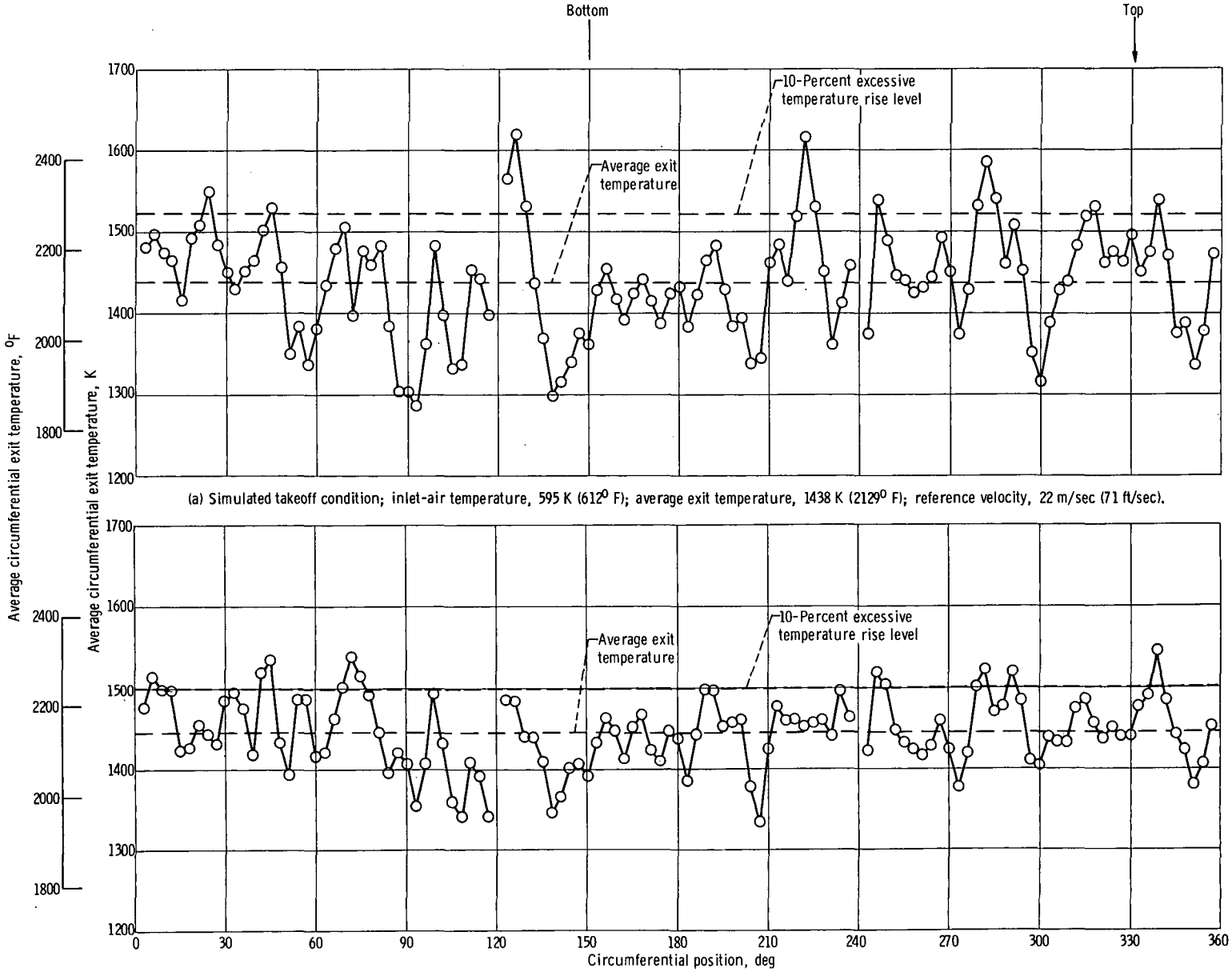

(a) Simulated takeoff condition; inlet-air temperature, 595 K (612° F); average exit temperature, 1438 K (2129° F); reference velocity, 22 m/sec (71 ft/sec).

(b) Mach 3.0 cruise condition; inlet-air temperature, 897 K (1154° F); average exit temperature, 1445 K (2141° F); reference velocity, 33 m/sec (108 ft/sec).

Figure 12. - Average circumferential temperature profiles. Nominal inlet-air total pressure, 62 N/cm^2 (90 psia).

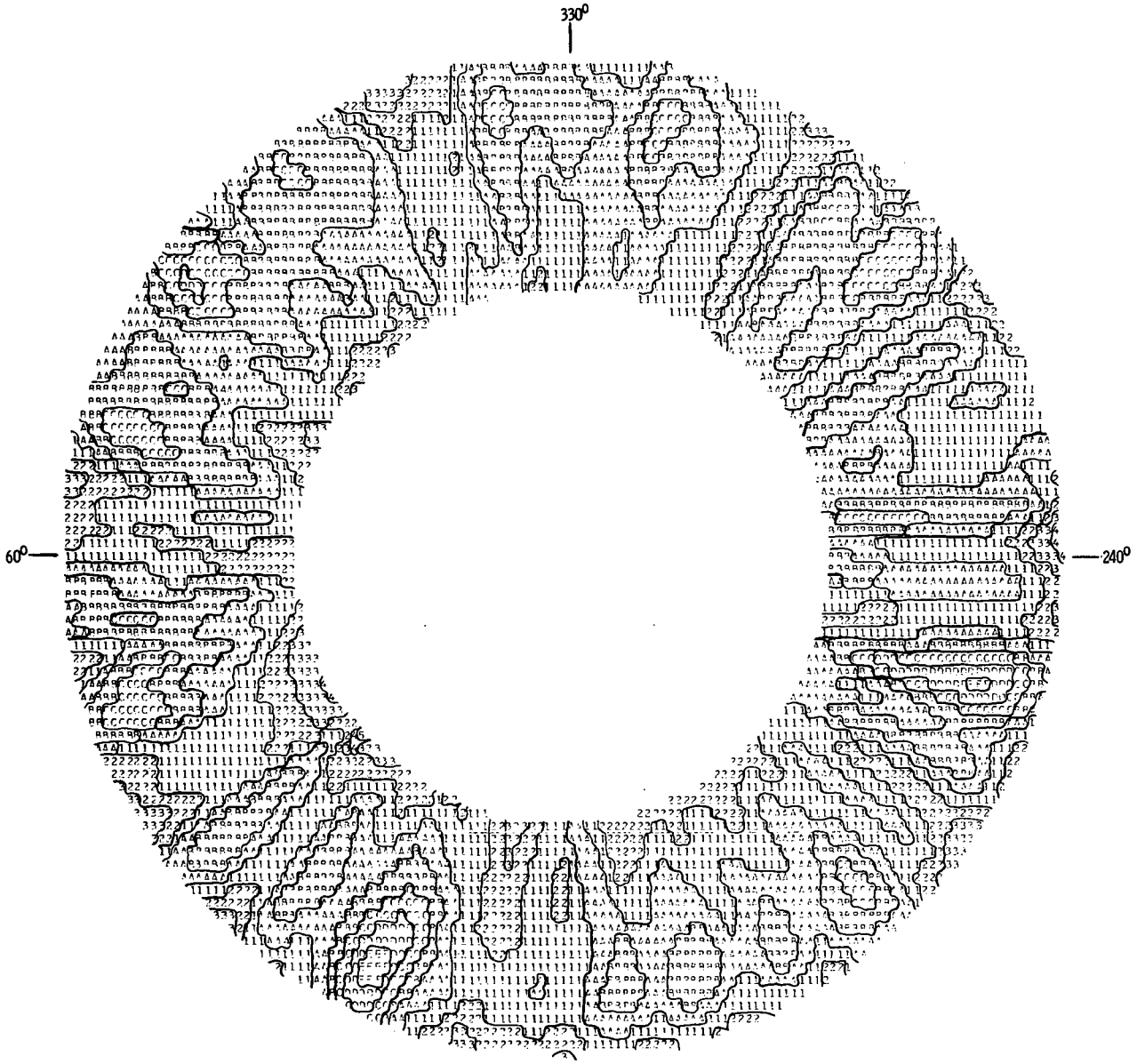

(a) Simulated takeoff condition: inlet-air temperature, 595 K (612° F); average exit temperature, 1436 K (2124° F); reference velocity, 22 m/sec (71 ft/sec).

Figure 13. - Combustor exit-temperature patterns. Nominal inlet-air total pressure, 62 N/cm^2 (90 psia). View looking upstream.

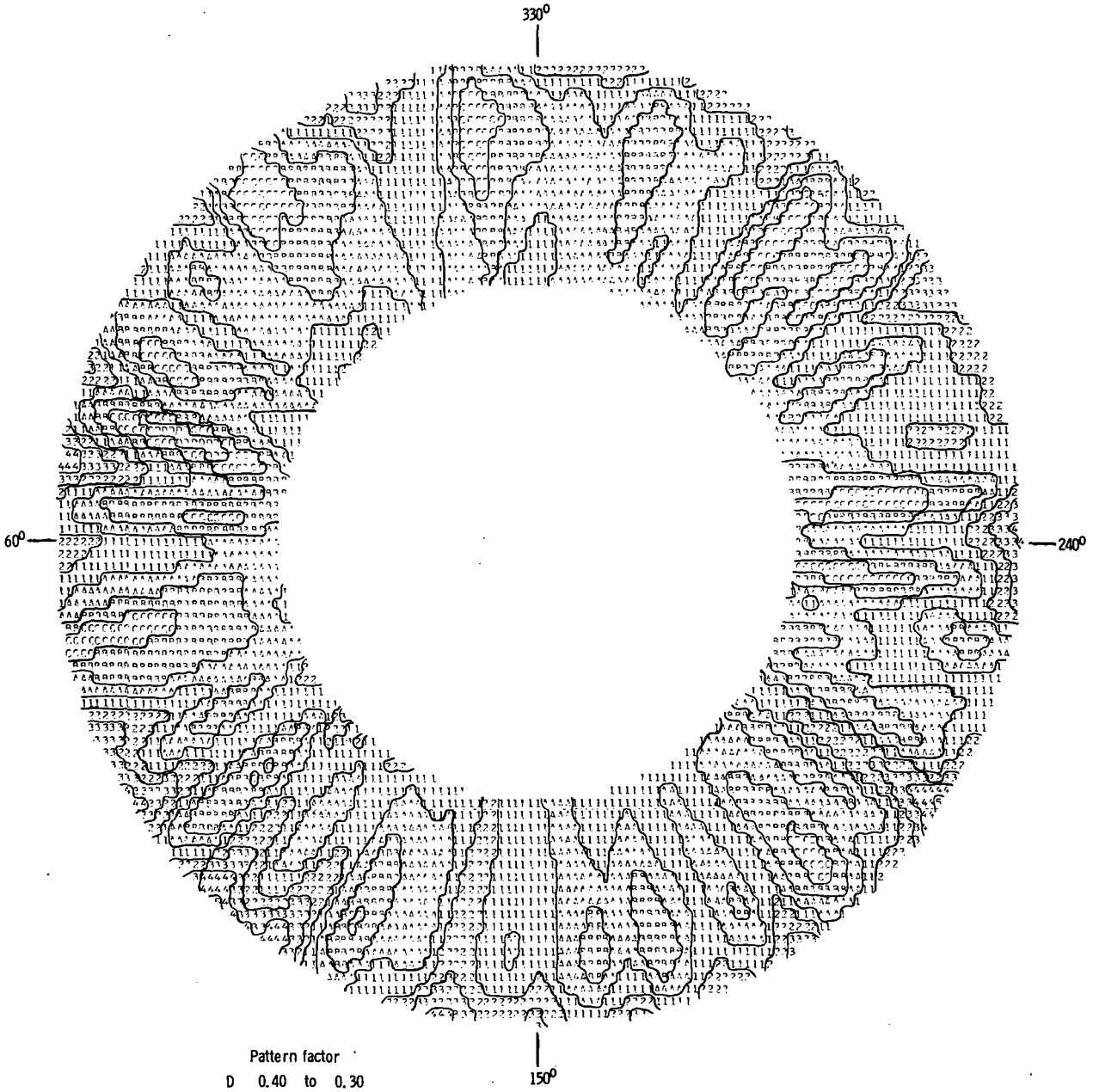

(b) Mach 3.0 cruise condition: inlet-air temperature, 897 K (1154° F); average exit temperature, 1450 K (2151° F); reference velocity, 33 m/sec (108 ft/sec).

Figure 13. - Concluded.

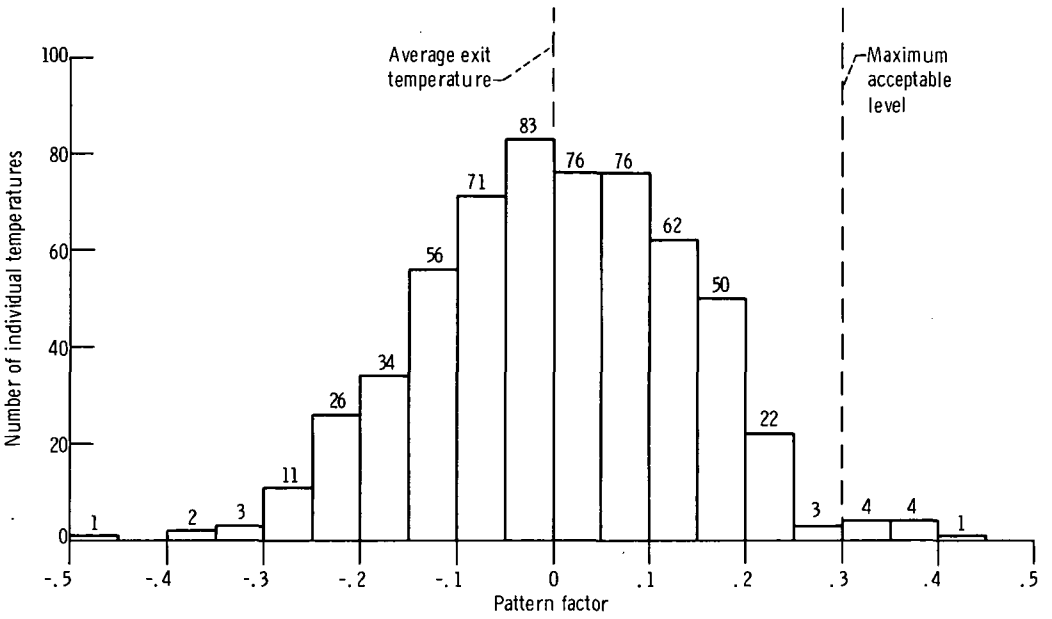

Figure 14. - Exit-temperature distribution by pattern factor range. Simulated takeoff conditions: inlet-air total pressure, 62 N/cm^2 (90 psia); inlet-air temperature, 590 K (600^0 F); average exit temperature, 1436 K (2124^0 F); reference velocity, 22 m sec (71 ft/sec). Number of individual temperatures out of 585 is indicated above each group. Reading 357, table III.

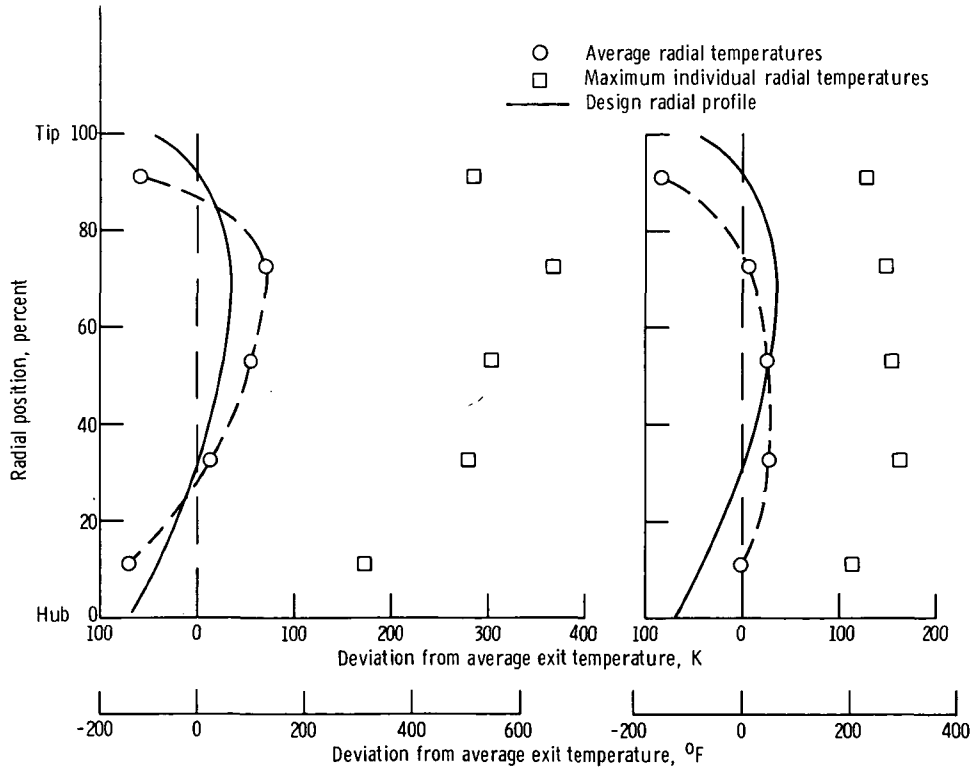

(a) Simulated takeoff condition: inlet-air temperature, 595 K (612^0 F); average exit temperature, 1436 K (2124^0 F); reference velocity, 22 m/sec (71 ft/sec). Run 357, table III.

(b) Mach 3.0 cruise condition: inlet-air temperature, 897 K (1154^0 F); average exit temperature, 1450 K (2151^0 F); reference velocity, 33 m/sec (108 ft/sec). Run 373, table III.

Figure 15. - Radial exit-temperature profile characteristics. Inlet-air total pressure, 62 N/cm^2 (90 psia).

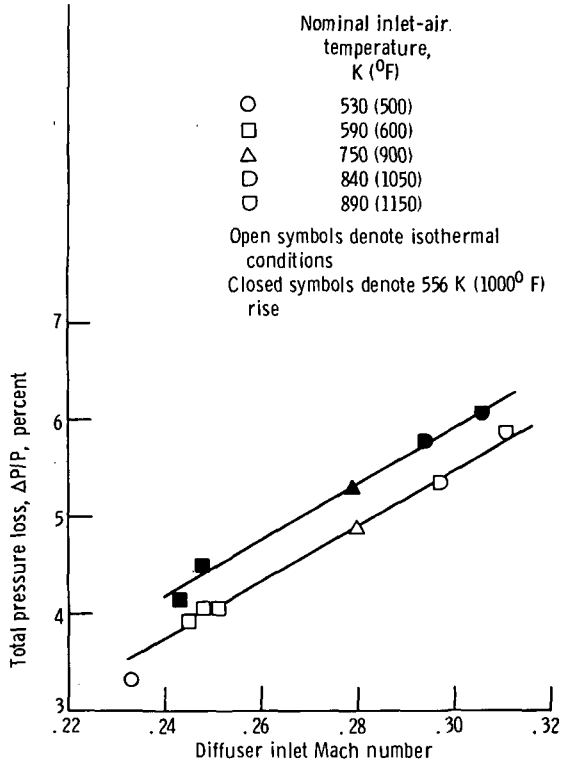

Figure 16. - Variation of combustor total pressure loss with diffuser inlet Mach number. Inlet-air pressure, 62 N/cm^2 (90 psia).

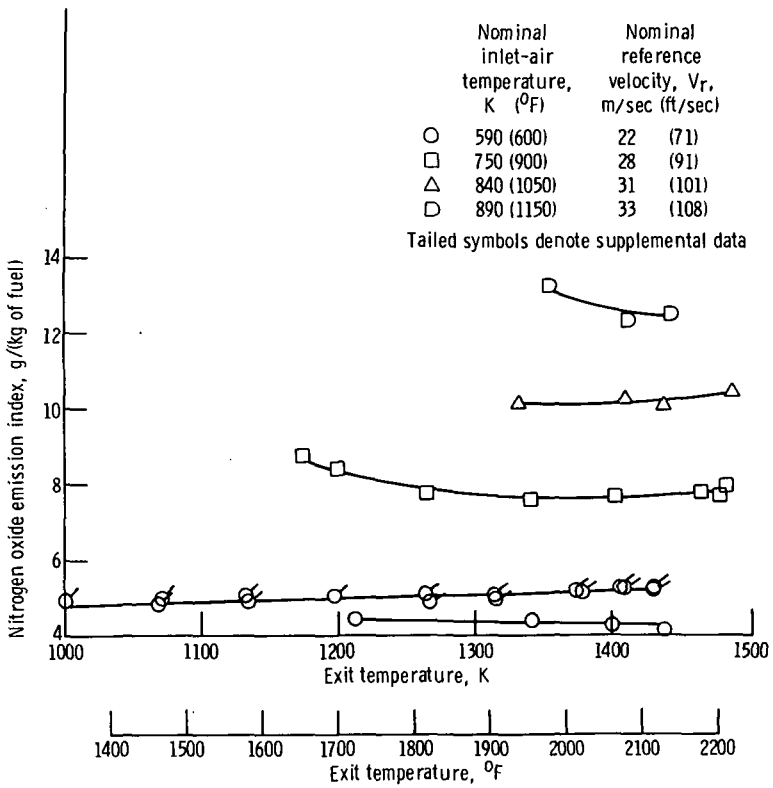

Figure 17. - Effect of combustor exit temperature on nitrogen oxide emission at various inlet temperatures and nominal inlet pressure of 62 N/cm^2 (90 psia).

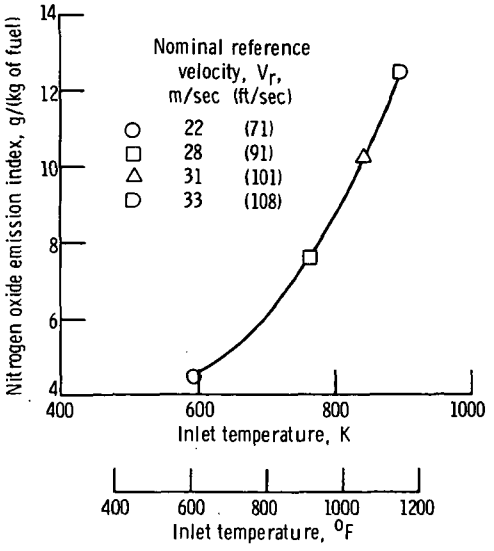

Figure 18. - Effect of combustor inlet temperature on nitrogen oxide emissions at nominal fuel-air ratio of 0.016 and inlet pressure of 62 N/cm^2 (90 psia).

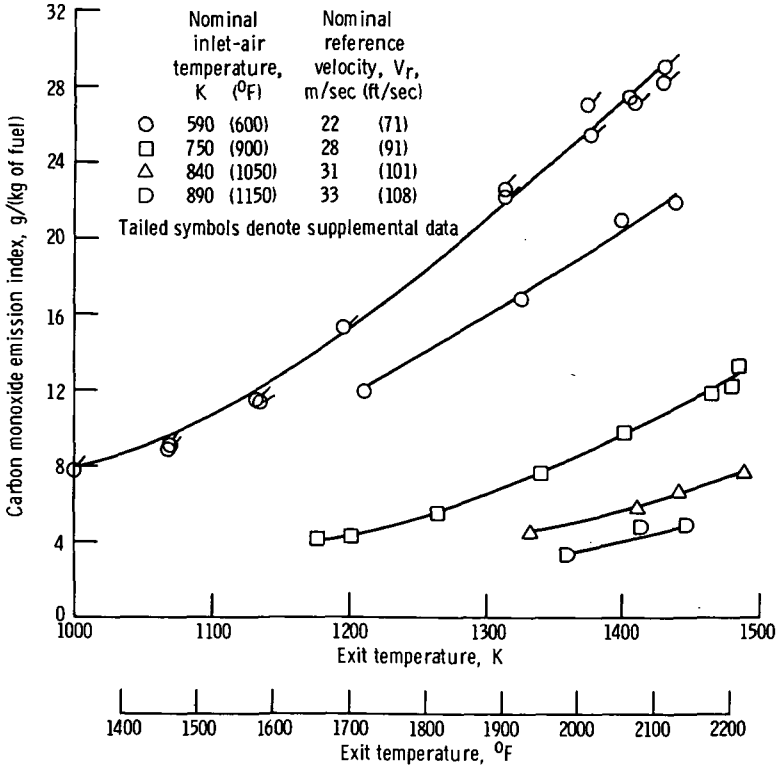

Figure 19. - Effect of combustor exit temperature on carbon monoxide emissions at various inlet temperatures and nominal inlet pressure of 62 N/cm^2 (90 psia).

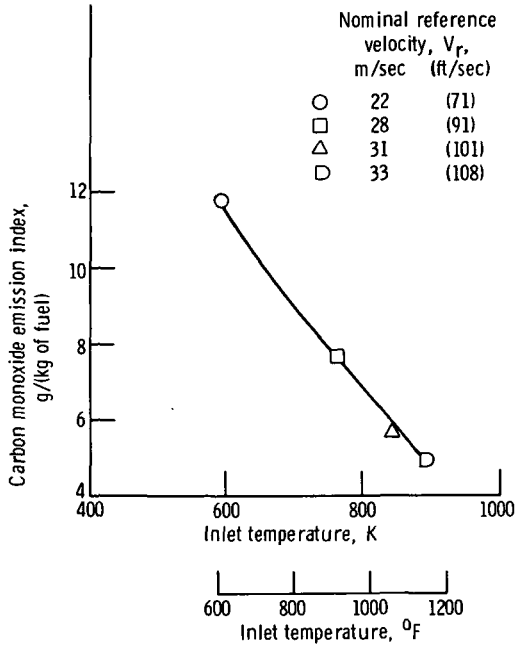

Figure 20. - Effect of combustor inlet-air temperature on carbon monoxide emission at nominal fuel-air ratio of 0.016 and inlet pressure of 62 N/cm^2 (90 psia).

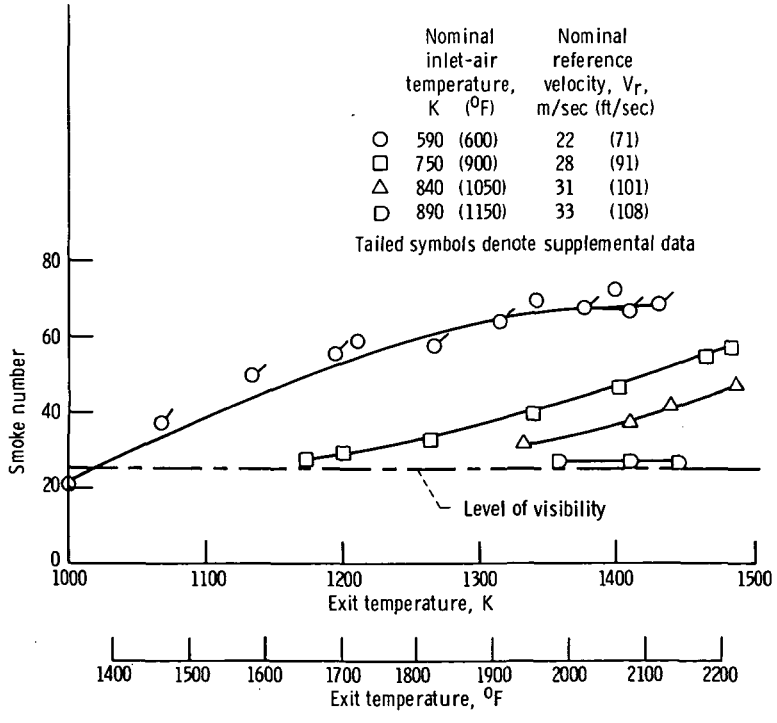

Figure 21. - Effect of combustor exit temperature on smoke number at various inlet-air temperatures and nominal inlet pressure of 62 N/cm^2 (90 psia).

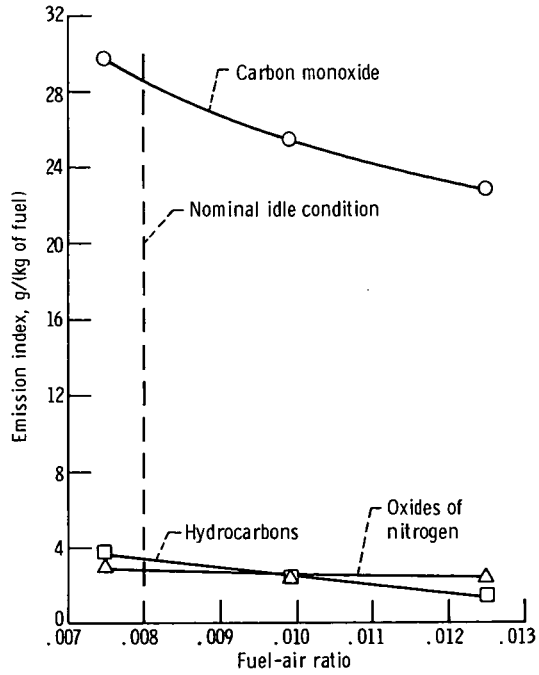

Figure 22. - Pollution levels at simulated engine idle conditions of 41-N/cm^2 (60 psia) inlet pressure, 480 K (400^0 F) inlet temperature, and 19-m/sec (64-ft/sec) reference velocity.

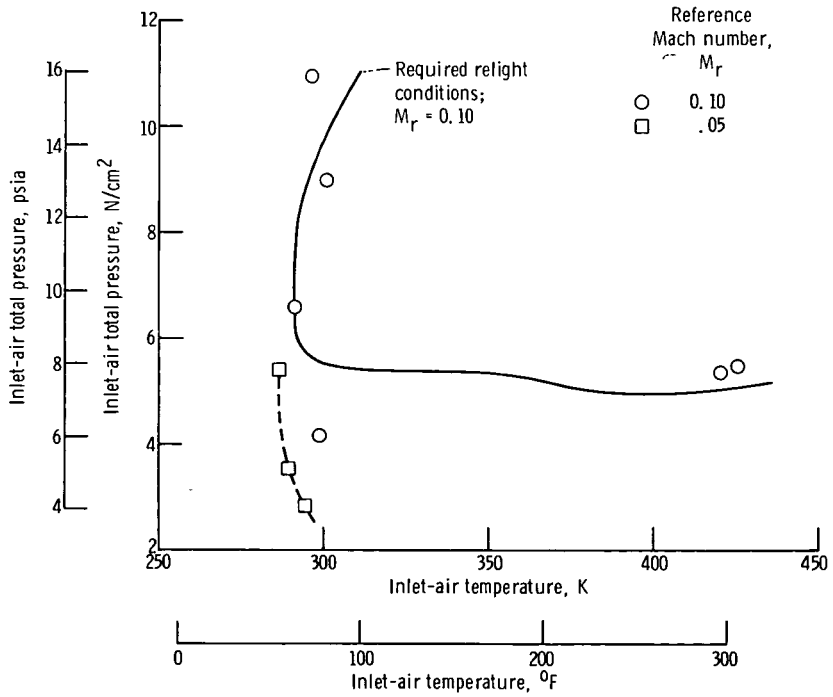

Figure 23. - Altitude relight performance of side-entry combustor. Data from table V(a).

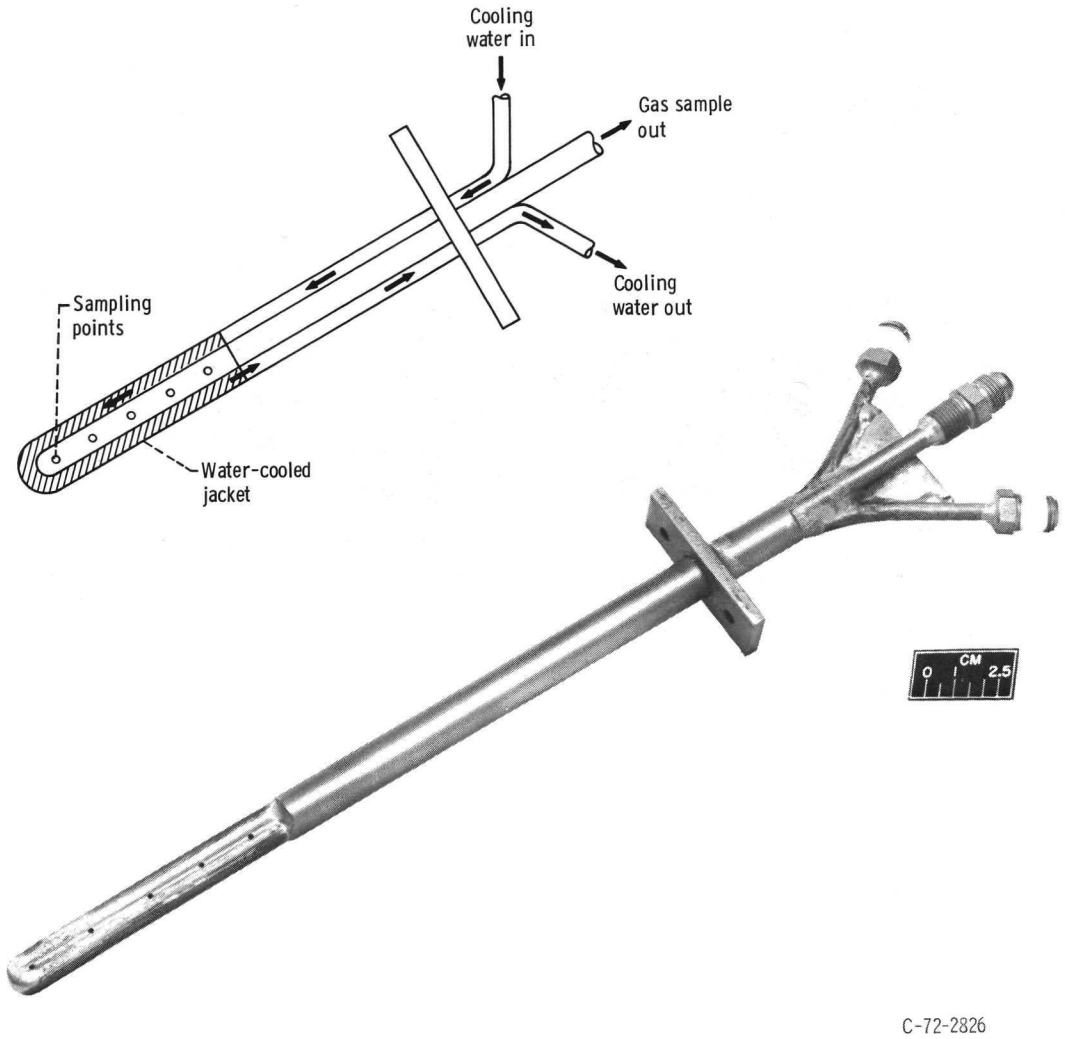

Figure 24. - Gas sampling probe.

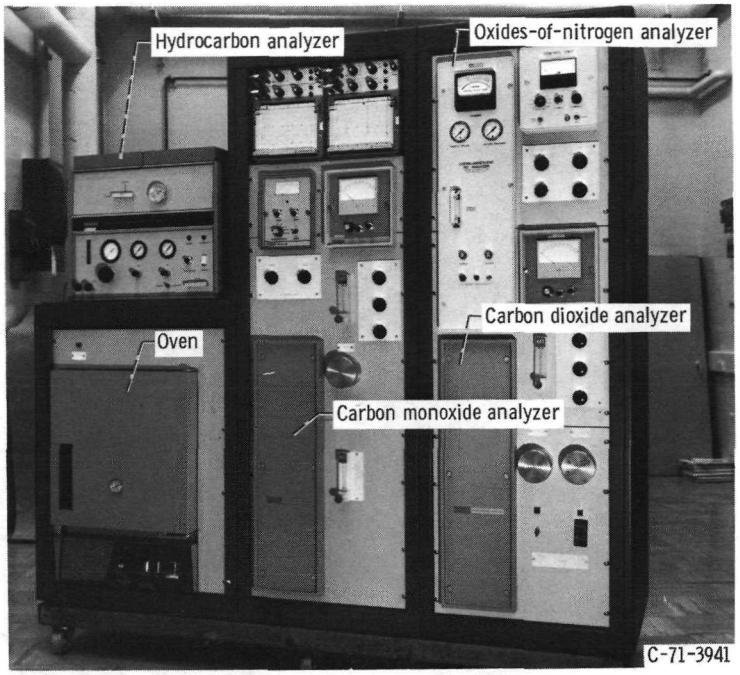

Figure 25. - Gas sampling instrument console.

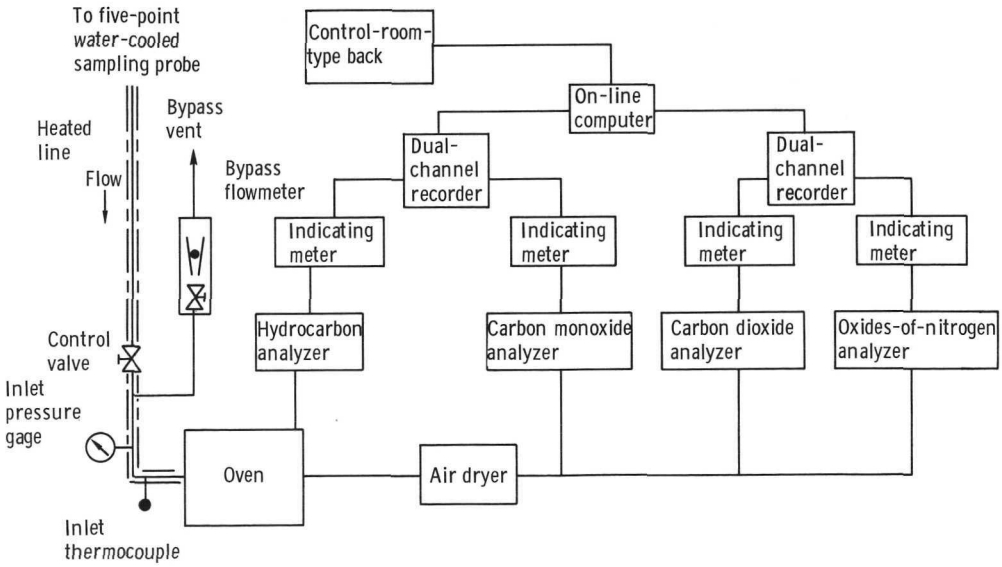

Figure 26. - Schematic diagram of gas analysis system.

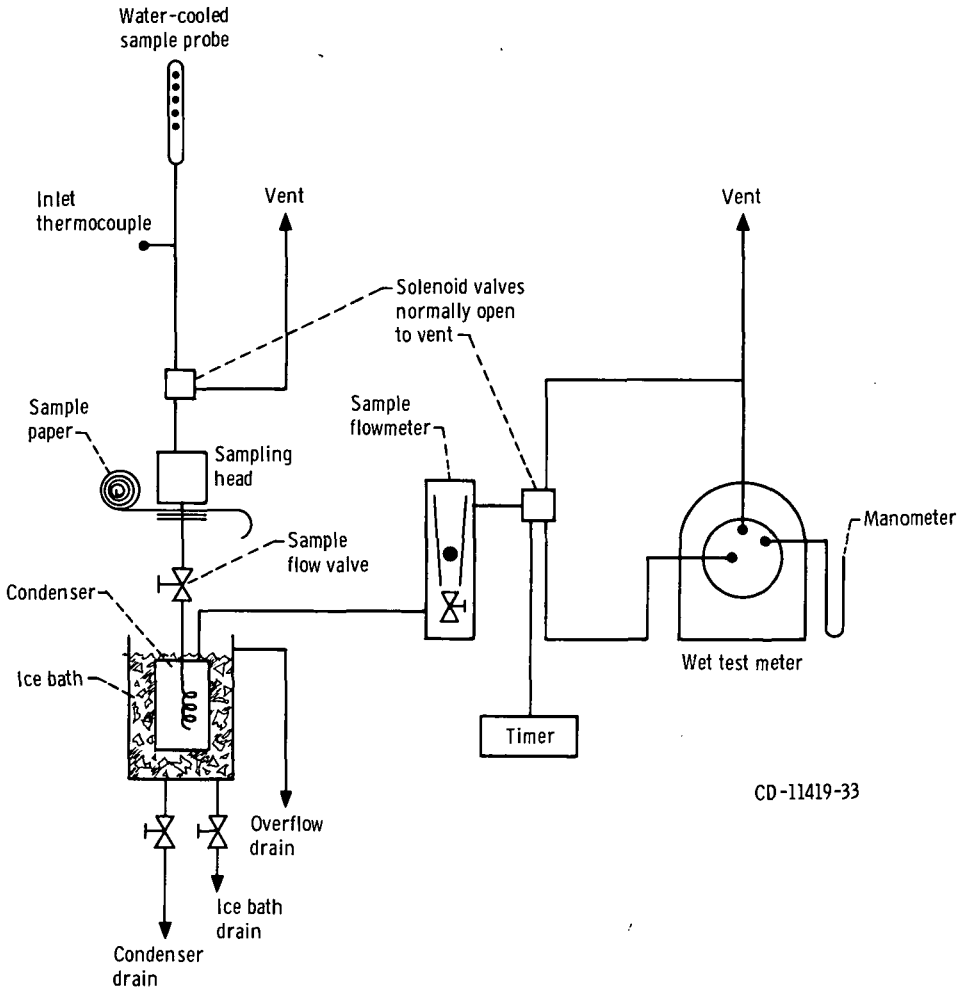

Figure 27. - Schematic flow diagram of smoke measurement system.

NATIONAL AERONAUTICS AND SPACE ADMINISTRATION
WASHINGTON, D.C. 20546

OFFICIAL BUSINESS
PENALTY FOR PRIVATE USE $300

SPECIAL FOURTH-CLASS RATE BOOK

POSTAGE AND FEES PAID
NATIONAL AERONAUTICS AND SPACE ADMINISTRATION
451

U.S.MAIL

POSTMASTER: If Undeliverable (Section 158 Postal Manual) Do Not Return

"The aeronautical and space activities of the United States shall be conducted so as to contribute . . . to the expansion of human knowledge of phenomena in the atmosphere and space. The Administration shall provide for the widest practicable and appropriate dissemination of information concerning its activities and the results thereof."

—NATIONAL AERONAUTICS AND SPACE ACT OF 1958

NASA SCIENTIFIC AND TECHNICAL PUBLICATIONS

TECHNICAL REPORTS: Scientific and technical information considered important, complete, and a lasting contribution to existing knowledge.

TECHNICAL NOTES: Information less broad in scope but nevertheless of importance as a contribution to existing knowledge.

TECHNICAL MEMORANDUMS: Information receiving limited distribution because of preliminary data, security classification, or other reasons. Also includes conference proceedings with either limited or unlimited distribution.

CONTRACTOR REPORTS: Scientific and technical information generated under a NASA contract or grant and considered an important contribution to existing knowledge.

TECHNICAL TRANSLATIONS: Information published in a foreign language considered to merit NASA distribution in English.

SPECIAL PUBLICATIONS: Information derived from or of value to NASA activities. Publications include final reports of major projects, monographs, data compilations, handbooks, sourcebooks, and special bibliographies.

TECHNOLOGY UTILIZATION PUBLICATIONS: Information on technology used by NASA that may be of particular interest in commercial and other non-aerospace applications. Publications include Tech Briefs, Technology Utilization Reports and Technology Surveys.

Details on the availability of these publications may be obtained from:

SCIENTIFIC AND TECHNICAL INFORMATION OFFICE

NATIONAL AERONAUTICS AND SPACE ADMINISTRATION

Washington, D.C. 20546